Rationality, irrationality and escalating behavior in lowest unique bid auctions

Filippo Radicchi,[1,2,3] Andrea Baronchelli,[4] and Luís A. N. Amaral[1,2,5]

[1]*Howard Hughes Medical Institute (HHMI), Northwestern University, Evanston, Illinois 60208 USA*
[2]*Department of Chemical and Biological Engineering, Northwestern University, Evanston, Illinois 60208 USA*
[3]*Departament d'Enginyeria Quimica, Universitat Rovira i Virgili, Av. Paisos Catalans 26, 43007 Tarragona, Catalunya, Spain*
[4]*Departament de Física i Enginyeria Nuclear, Universitat Politècnica de Catalunya, Campus Nord B4, 08034 Barcelona, Spain*
[5]*Northwestern Institute on Complex Systems (NICO), Northwestern University, Evanston, Illinois 60208 USA*

Information technology has revolutionized the traditional structure of markets. The removal of geographical and time constraints has fostered the growth of online auction markets, which now include millions of economic agents worldwide and annual transaction volumes in the billions of dollars. Here, we analyze bid histories of a little studied type of online auctions — lowest unique bid auctions. Similarly to what has been reported for foraging animals searching for scarce food, we find that agents adopt Lévy flight search strategies in their exploration of "bid space". The Lévy regime, which is characterized by a power-law decaying probability distribution of step lengths, holds over nearly three orders of magnitude. We develop a quantitative model for lowest unique bid online auctions that reveals that agents use nearly optimal bidding strategies. However, agents participating in these auctions do not optimize their financial gain. Indeed, as long as there are many auction participants, a rational profit optimizing agent would choose not to participate in these auction markets.

Introduction

Animals searching for scarce food resources display movement patterns that can be statistically classified as Lévy flights [1–8]. Lévy flights [9] represent the best strategy that can be adopted by a searcher looking for a scarce resource in an unknown environment [10], and foraging animals seem therefore to have learned the best strategy for survival. Lévy flights describe also the movement patterns of humans in real space [11] and the variability of economic indices [12], but these observations do not correspond to search processes as in the case of foraging animals. Surprisingly, there is no indication of whether humans also use Lévy flight strategies when searching for scarce resources. Analyzing apparently unrelated data regarding online auctions, we address here this question and show that, when searching for scarce resources, humans explore the relevant space in the same class of strategies as foraging animals do.

Lowest unique bid auctions are a new generation of online markets [13–18]. Agents winning lowest unique bid auctions may purchase expensive goods for absurdly low prices; cars, boats and even houses can be bought for only hundreds of dollars. The idea of the auction is strikingly simple. A good, typically with a market value V of at least a thousand dollars, is put up for auction. The auction duration is fixed *a priori*. A bid can be any amount from one cent to a pre-determined maximum value M, generally lower than one hundred dollars. Each time an agent makes a bid on a value $1 \leq b \leq M$, she pays a fee c, which ranges from one to ten dollars depending on the auction. During the bidding period, an agent knows only the status of her new bid, that is, whether it is winning or not. None of the agents knows on what values the other agents have bid until the end of the auction. When the bidding period expires, the agent who made the lowest unmatched bid can purchase the good for the value of the winning bid (see Fig. 1 for an illustration of the determination of the winning bid).

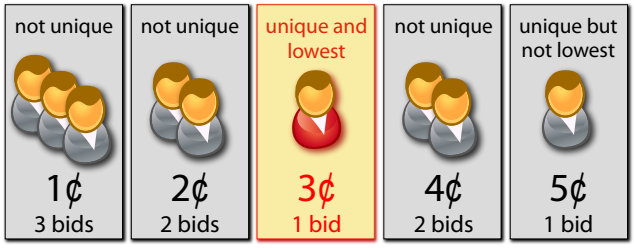

Figure 1: **Unique bid auctions.** Illustration of the rules of a lowest unique bid auction. At the end of the auction, the winner results to be the agent who has bid $3¢$, which represents the lowest unique bid. All other bids are not unique apart from the one of $5¢$, which is not the lowest one. In highest unique bid auctions the mechanism is reversed, and the winner is the agent making the highest unmatched bid. Illustration of the rules of a lowest unique bid auction. At the end of the auction, the winner results to be the agent who has bid $3¢$, which represents the lowest unique bid. All other bids are not unique apart from the one of $5¢$, which is not the lowest one. In highest unique bid auctions the mechanism is reversed, and the winner is the agent making the highest unmatched bid.

Lowest unique bid auction markets are competitive arenas. Each agent performs a search for a single target whose position changes from auction to auction, as it is determined by the bid history of the whole population of agents. Since the cost of each bid is as much as 100 times larger than the natural unit of the bid, the number of bids that can be made by a single agent is limited and allows only a partial exploration of the bid space. Successful agents need to identify good strategies in order to maximize their winning chances and thus limit their risk.

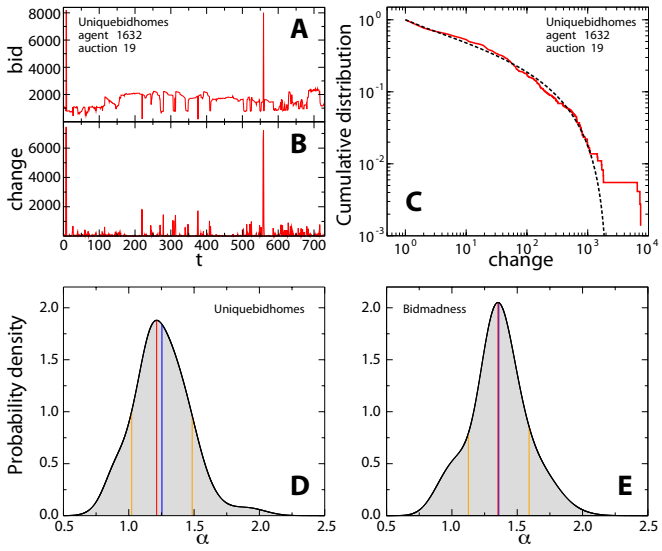

Figure 2: **Individual activity.** **(A)** Bid values explored by agent 1632 on auction 19 in the data set `www.uniquebidhomes.com`. Bids are sorted chronologically, and the figure reports the value b_t of the t-th bid. The unit of the bid amount is one hundredth of an Australian dollar. **(B)** Absolute value of the difference between two consecutive bids. The exploration of the bid space is characterized by a bursty behavior, where many small movements are occasionally followed by large jumps. **(C)** Cumulative distribution function of the change in bid value. The distribution is well fitted by a power-law, with decay exponent consistent with $\alpha = 1.3 \pm 0.1$ (dashed line). The agent therefore explores the bid space using a Lévy flight strategy. Notice that the curve bends down because of the finiteness of the bid space. **(D)** Probability density function of the Lévy-flight exponents adopted by agents in lowest unique bid auctions (`www.uniquebidhomes.com`). The blue line indicates the average value $\langle\alpha\rangle \simeq 1.26$ of the distribution, the red line identifies the mode $\alpha_b \simeq 1.21$ of the distribution, the orange lines bound the region within one standard deviation $\sigma \simeq 0.23$ from the average. **(E)** Probability density function of the Lévy-flight exponents adopted by agents in highest unique bid auctions (`www.bidmadness.com.au`). In this case we find $\langle\alpha\rangle \simeq 1.36$, $\alpha_b \simeq 1.35$ and $\sigma \simeq 0.23$.

Lowest unique bid auctions are just a particular variant of online pay-to-bid auctions, but other types of pay-to-bid auctions are regularly hosted on the web. For example, in highest unique bid auction the mechanism of lowest unique bid auction is inverted, and the winning bid is determined by the highest value closest to a pre-determined upper bound value. Since these auctions still involve a blind search of the winning value, highest unique bid auctions are equivalent to lowest unique bid auctions. Indeed, in this paper we analyze data taken from both types of auctions.

Other online pay-to-bid auctions, however, can be very different from lowest unique bid auctions. For example, the so-called penny auctions, which have acquired a great popularity in recent years, appear quite similar to but are not. As in the case of lowest unique bid auctions, the cost of the fee is at least 100 times larger of the bid increment, and as a consequence, the final value of the winning bid is much lower than the real value of the good up for auction. However, in penny auctions the value of the winning bid is publicly known and can only grow during the auction (i.e., the word "penny" is used because, in penny auctions, bid increments are equal to one cent). While escalation plays a very important role in penny auctions, in this type of auctions agents do not need to explore the bid space because the value of the winning bid is known. Penny auctions have been the focus of some theoretical and empirical studies [19–23].

Results

We collected data from three distinct web sites hosting lowest unique bid auctions. We automatically downloaded and parsed the content of the tables reporting the bid history of closed auctions. These data sets contain all the information on individual auctions, including the details of each bid: its value, when it was made and who placed it. These data allow us to keep track of all the movements performed on bid space by a given agent bidding in a specific auction.

We show in Figure 2A a typical exploration of the bid space performed by a single agent. The exploration of the bid space is bursty: consecutive bid values are generally close to each other, but from time to time the agent performs "long jumps" in bid space. We first compute the jump lengths (Fig. 2B) and estimate their probability distribution function (Fig. 2C). We find a strikingly robust power-law scaling consistent with the exploration of the bid space using a Lévy flight search strategy [9]. Note that here we use the notion of discrete Lévy flights. Time and space are in fact discrete, and the exploration of the bid space is modeled as a discrete time Markov chain [with transition probability defined in Eq. 8]. Our discrete model converges to a standard Lévy flight only in the continuum limit of space and time [24]. The power-law scaling can be observed both at the level of single agents (whenever the number of bids is sufficiently large for estimating the distribution; c.f. Figs. 2C and Supporting Information) and globally, by aggregating the length of the jumps made by all agents in all auctions (Figs. 3A and Supporting Information). The density distribution of the exponents calculated over single agents is peaked around a mean value $\langle\alpha\rangle \simeq 1.3$ (Figs. 2D, 2E and Supporting Information), the same exponent value we estimate for the aggregated data. Significant variations around the average value are anyway present, and reflect the heterogeneity of the agent strategies. The density distributions of Figs. 2D and 2E are in fact calculated by considering different agents bidding in different auctions.

The power-law scaling and its measured exponent are very stable. Exponent estimates do not depend on the direction of the jumps (Figs. 3B and Supporting Information) or the level of activity of the agent (Figs. 3C and Supporting Information). Surprisingly, performing Lévy flights does not appear to be a learned strategy. Instead it appears to be an intrinsic feature of the mental search process: the jump lengths in the bid space follow the same power-law at any stage of the auction

(Figs. 3D and Supporting Information).

Our results represent the strongest empirical evidence for the use of Lévy flight strategies in the search of scarce resources reported in literature up to now. Differently from previous studies where "two orders of magnitude of scaling can represent a luxury" [6], here the power-law decay can be clearly observed even over four orders of magnitude. It is unlikely, though, that adopting Lévy flight strategies is a deliberate choice of the agents, just as it is not likely that animals searching for food consciously follow a Lévy flight strategy. Nevertheless, the data demonstrate that the changes in bid value are statistically consistent with a power-law decaying distribution over several orders of magnitude (see and Supporting Information) [25]. Simple correlation measurements show also that the lengths of consecutive jumps are independent of each other (see and Supporting Information). We believe that the power-law is valid over such a broad regime because the space is not strictly physical. That is, movements of tens of thousands of cents can be performed for the same cost of those of only one cent. Agents thus explore the bid space in an effectively super-diffusive fashion, and steps are made with infinite velocity.

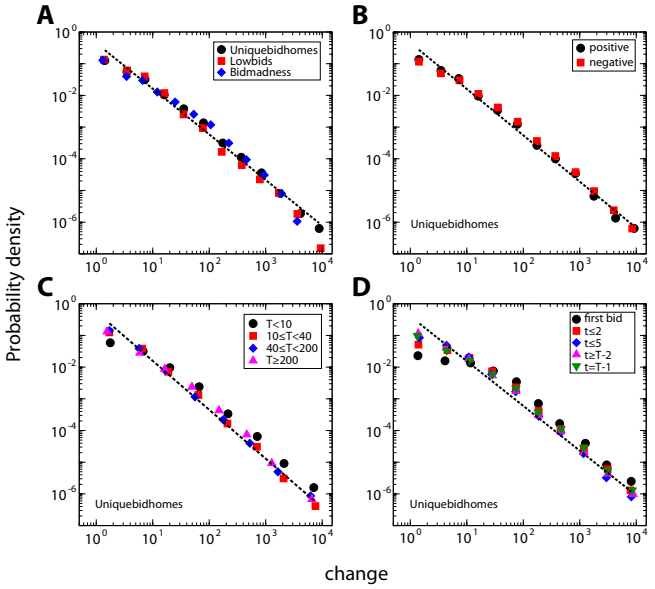

Figure 3: **Bidding strategies of agents are Lévy flights. (A)** Probability density function of the bid change for all agents in all auctions. We analyze data sets from three different web sites hosting auctions: `www.uniquebidhomes.com` (black circles), `www.lowbids.com.au` (red squares) and `www.bidmadness.com.au` (blue diamonds). **(B)** Probability density function of positive (black circles) and negative (red squares) bid changes. **(C)** Probability density function of the change amount for data aggregated over agents with different levels of activity (T indicates the total number of bids made by an agent in a single auction). **(D)** Probability density function of the change amount at different stages of the auctions (t stands for order of the bid change in the bid history of an agent). In (A), (B) and (D) results have been obtained for lowest unique bid auctions (`www.uniquebidhomes.com`). All dashed lines stand for best power-law fits (least square) and all exponent values are consistent with $\alpha = 1.4 \pm 0.1$. The unit of the bid value change amount is one hundredth of an Australian dollar.

Model

Next, we model the lowest unique bid auction process. Consider N agents competing in a lowest unique bid auction. We model the successive bids of these agents as Lévy flight searches on bid space. Each agent moves in a bounded one-dimensional lattice with an *a priori* chosen exponent value, which may be regarded as the agent's strategy in the auction. In our formulation, every agent performs the same number T of bids and may return to already visited sites. At the beginning of the auction, every agent sits at the leftmost site on the lattice and then performs T movements by changing, at each step, her actual position by an amount randomly drawn from a power-law distribution. If at stage $t-1$ the agent with strategy α is sitting at position j, then at stage t she jumps to position i with probability proportional to $|i-j|^{-\alpha}$. This model provides us with an independent way to determine the exponent values of the Lévy flights and offers a strikingly good statistical description of the data (Fig. 2B and Supporting Information).

We focus our attention on a generic agent bidding with strategy β and on her chances to win auctions in which the rest of the population is bidding with strategy γ. More complicated situations may in principle be studied with the same formalism.

Single bid

Consider first the case in which agents make a single bid. The probability that a generic opponent, using bidding strategy γ, bids on value i is

$$p_\gamma(i) = i^{-\gamma}/m(\gamma) \quad , \tag{1}$$

with $m(\gamma) = \sum_{j=1}^{M} j^{-\gamma}$ proper normalization constant. Here we consider the simple case in which all agents adopt the same bidding strategy γ. The probability of Eq. (1) can be anyway made more general by assuming that agents chose strategies from a density distribution $g(\alpha)$ and calculating the probability of Eq. 1 as $p(i) = \int d\alpha \; i^{-\alpha}/m(\alpha) \;\; g(\alpha)$. After all agents have bid, there will be n_k bids on the k-th bid value. Such variables clearly obey the constraint $N = \sum_{k=1}^{M} n_k$. The probability to observe a particular configuration $\{n\} = (n_1, n_2, \ldots, n_k, \ldots, n_M)$ is given by

$$P_\gamma(\{n\}) = N! \prod_{k=1}^{M} \frac{[p_\gamma(k)]^{n_k}}{n_k!} \quad , \tag{2}$$

which is a multinomial distribution with weights given by Eq. (1). In particular, the probability that only one bid (i.e.,

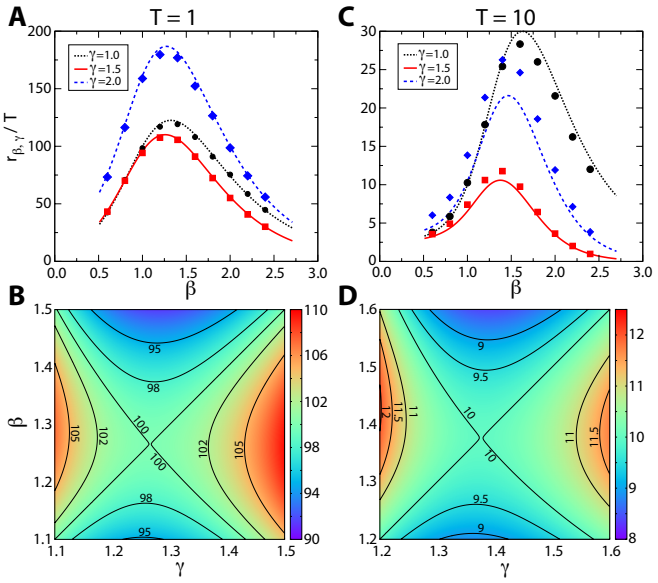

Figure 4: **Model predictions.** Economic return $r_{\beta,\gamma}$ [Eq. (7)], divided by the number of bids T, of an agent bidding with strategy β when competing, in a lowest unique bid auction with upper-bound $M = 1,000$ and for a good of value $V = 10,000$, against $N = 100$ opponents bidding with strategy γ. Unless specified, the quantity $r_{\beta,\gamma}$ reported in this plots is computed by numerically solving the equations of the model. **(A)** Case where each agent performs a single bid in the auction, for three values of γ. Theoretical predictions (lines) are compared with the results of numerical simulations (symbols). In each simulation of the auction, we randomly extracted N bid values j with probability proportional to $j^{-\gamma}$, and a single bid value v with probability proportional to $v^{-\beta}$. For a given set of parameters, we repeated the same simulation $G = 10,000$ times, and calculate the number of times g in which the bid value extracted from the power-law distribution with exponent β was the winning bid, and the sum I of these winning bid values. The economic return has been finally calculated as $r_{\beta,\gamma} = (gV - I)/G$. **(B)** Exploration of parameter space reveals the existence of a saddle point at $\beta_s = \gamma_s \simeq 1.27$. **(C)** Case where each agent performs 10 bids in the auction, for three values of γ. Numerical simulations have been carried out as in the former case, but considering agents moving in the bid space according to Eq. (8). **(D)** Exploration of parameter space reveals the existence of a saddle point at $\beta_s = \gamma_s \simeq 1.38$.

a unique bid) is made on value i is

$$u_\gamma(i) = P_\gamma(n_i = 1) = \sum_{\sum_{k\neq i} n_k = N-1} P_\gamma(\{n\}) = N p_\gamma(i) [1 - p_\gamma(i)]^{N-1} \quad . \quad (3)$$

Focus now on the agent with bidding strategy β. The probability that, making a bid on value v, she makes a lowest unique bid can be calculated exactly by summing the multinomial distribution of Eq. (2) over all configurations for which there are no bids on the value v and there is not a unique bid on a value smaller than v, and finally multiplying this factor by the probability that the agent with bidding strategy β bids on the value v. Such exact calculation is however unfeasible due to the extremely high number of possible combinations, and therefore we approximate the probability that, making a bid on value v, the agent with bidding strategy β makes a lowest unique bid as

$$l_{\beta,\gamma}(v) = p_\beta(v) [1 - p_\gamma(v)]^N \prod_{k<v} [1 - u_\gamma(k)] \quad . \quad (4)$$

The r.h.s. of Eq. (4) is the product of three terms: $p_\beta(v)$ is the probability that the agent bids on value v; $[1 - p_\gamma(v)]^N$ is the probability that none of the opponents have bid on value v; $\prod_{k<v} [1 - u_\gamma(k)]$ is the probability that none of the bid values smaller than v are occupied by a single bid made by one of the opponents. In spite of the fact that Eq. (4) is just an approximation of the real $l_{\beta,\gamma}(v)$, the approximation can be considered good because able to reproduce the results obtained from the direct simulation of the process (see the section Results). Moreover in the simplest case in which $N = 1$, it correctly reduces to the exact value $l_{\beta,\gamma}(v) = p_\beta(v) \prod_{k\leq v} [1 - p_\gamma(k)]$.

Finally, the probability that the agent with bidding strategy β wins the auction is

$$w_{\beta,\gamma} = \sum_{v=1}^{M} l_{\beta,\gamma}(v) \quad (5)$$

and, on average, the value of her winning bid is

$$\langle v \rangle_{\beta,\gamma} = \sum_{v=1}^{M} v\, l_{\beta,\gamma}(v) \quad . \quad (6)$$

Repeated auctions

Imagine now to repeat the same auction G independent times. The probability that the agent bidding with strategy β wins g times out of G total auctions is given by a binomial distribution

$$P_{\beta,\gamma}(g) = \binom{G}{g} (w_{\beta,\gamma})^g (1 - w_{\beta,\gamma})^{G-g} \quad .$$

If the agent with bidding strategy β wins g auctions, the sum of her winning bids is a random variable I whose probability is determined by

$$R_{\beta,\gamma}(I|g) = \sum_{v_1+v_2+\ldots+v_g=I} l_{\beta,\gamma}(v_1)\, l_{\beta,\gamma}(v_2) \cdots l_{\beta,\gamma}(v_g) \quad ,$$

where the sum runs over the integer indices v_1, v_2, ..., v_g with the constraint that their sum should equal I. Excluding bidding costs, the average return of the agent in g victories is

$$r_{\beta,\gamma}(g) = (gV - I)/G \quad .$$

In general, the probability that the sum of the winning bids is equal to I in an arbitrary number of auctions won by the player with bidding strategy β can be calculated as

$$R_{\beta,\gamma}(I) = \sum_g P_{\beta,\gamma}(g)\, R_{\beta,\gamma}(I|g) \quad ,$$

and a similar expression can be derived for the distribution of $r_{\beta,\gamma}(g)$. However, we are interested in the case in which the number of auctions diverges ($G \gg 1$). In this limit, we can approximate the number of victories with its average $\langle g \rangle = G\, w_{\beta,\gamma}$ as well as the sum of the winning bids as $I = \langle g \rangle \langle v \rangle_{\beta,\gamma} = G\, w_{\beta,\gamma} \langle v \rangle_{\beta,\gamma}$. The return of the agent with bidding strategy β is therefore

$$r_{\beta,\gamma} = w_{\beta,\gamma} \left(V - \langle v \rangle_{\beta,\gamma} \right) \quad . \tag{7}$$

For $r_{\beta,\gamma} > c$, the agent has a positive return for participating in the auction, whereas, for $r_{\beta,\gamma} < c$, her return is negative.

Multiple bids

Given a generic agent with bidding strategy α, her first bid is placed on value i with probability $q_\alpha^{(1)}(i) = i^{-\alpha}/m(\alpha)$. For the subsequent bids, we need to define a transition matrix Q_α, whose generic element $(Q_\alpha)_{ji}$ gives the probability that the agent bids on value i when her previous bid has been made on value j. In our model, we have

$$(Q_\alpha)_{ji} = \frac{|i-j|^{-\alpha} \left[1 - \delta(i-j)\right]}{m_j(\alpha)} \quad , \tag{8}$$

for all i and j in the interval $[1, M]$. $\delta(\cdot)$ is the Kronecker delta, equal to one if its argument is equal to zero, and equal to zero otherwise. The normalization constant $m_j(\alpha) = \sum_{i=1, i\neq j}^{M} |i-j|^{-\alpha}$ ensures the proper definition of the transition matrix. The matrix Q describes a random walker performing uncorrelated Lévy flights with exponent α. Notice that the agent has no memory of her previous bid values and therefore she may place more than a bid on the same value. At the generic step t, the probability that the agent with bidding strategy α bids on the value i is

$$q_\alpha^{(t)}(i) = \sum_{j=1}^{M} (Q_\alpha)_{ji}\; q_\alpha^{(t-1)}(j) \quad .$$

The probability that this agent has bid, during her T bids, on value i is then

$$s_\alpha^{(T)}(i) = 1 - \prod_{t=1}^{T} \left[1 - q_\alpha^{(t)}(i) \right] \quad .$$

The term $1 - q_\alpha^{(t)}(i)$ counts the probability that the agent has not bid on value i at stage t. The probability that the agent has not bid on value i at any stage is therefore the product of this single step probabilities. Finally, the probability that the agent has bid on value i at least once is calculated as the probability to have bid on value i an arbitrary number of times minus the probability to have never bid on value i.

Now go back to the situation in which an agent with bidding strategy β is opposed to a population of N agents with bidding strategy γ. The probability that the agent with bidding strategy β has bid, in T steps, at least once on value i is $s_\beta^{(T)}(i)$. The probability that one of the N opponents, bidding with strategy γ, makes a unique bid on value i is given by

$$u_{\beta,\gamma}^{(T)}(i) = N\, s_\gamma^{(T)}(i) \left[1 - s_\gamma^{(T)}(i)\right]^{N-1} \left[1 - s_\beta^{(T)}(i)\right] \quad . \tag{9}$$

$u_{\beta,\gamma}^{(T)}(i)$ is the product of two terms: $N\, s_\gamma^{(T)}(i) \left[1 - s_\gamma^{(T)}(i)\right]^{N-1}$ is the probability that a bid on value i is unmatched by any of the other $N-1$ opponents, while $1 - s_\beta^{(T)}(i)$ is the probability that also the agent, with bidding strategy β, does not bid on value i. The probability that the agent with strategy β wins the auction with a bid on value v is

$$l_{\beta,\gamma}^{(T)}(v) = s_\beta^{(T)}(v) \left[1 - s_\gamma^{(T)}(v)\right]^{N} \prod_{k<v} \left[1 - u_{\beta,\gamma}^{(T)}(v)\right] \quad , \tag{10}$$

respectively standing for the product of the probabilities that: she bids on value v; none of the other agents bids on value v; none of the bids with value smaller than v is unique. Eqs. (9) and (10) represent the generalization of Eqs. (3) and (4), respectively. In Eq. (10) we made the same type of approximation as the one used for writing Eq. (4). The probability $w_{\beta,\gamma}^{(T)}$ that the agent with bidding strategy β wins the auction and the average value $\langle v \rangle_{\beta,\gamma}^{(T)}$ of her winning bids can be respectively calculated using Eqs. (5) and (6). Finally, excluding bidding costs, the return $r_{\beta,\gamma}$ of the agent with strategy β over an infinite number of auctions is again given by Eq. (7). For $r_{\beta,\gamma} > T\,c$, the agent has a positive return for participating in the auction, whereas, for $r_{\beta,\gamma} < T\,c$, her return is negative.

Model predictions

We show in Fig. 4 the results obtained with our analytical model. The presence of a saddle point at $\gamma_s = \beta_s$ indicates that β_s is an optimal strategy or Nash equilibrium [26–28]. When the opponents do not bid rationally (i.e., $\gamma \neq \gamma_s$), it is more convenient to use a strategy $\beta \neq \beta_s$. On the other hand, when the other agents bid rationally (i.e., $\gamma = \gamma_s$), there is no better strategy than β_s. The value of β_s depends on the parameters N and T , but for realistic choices (see and Supporting Information and Fig. 4), β_s is in the range 1.2 to 1.5, the same range of the exponent values we estimated from the data. Thus, despite its simplicity, our model captures the main features of the real auctions. Performing Lévy flights with small exponents (ballistic motion) yields unique bids that are unlikely to be the lowest. On the other hand, performing preferentially short jumps (high exponents, diffusive motion) guarantees to always bid on small values which are unlikely to be unique. Intermediate values of the exponent (super-diffusive motion) represent a compromise between staying low and being unique, and therefore lead to maximal winning chances. These considerations are valid only for finite values of N and T, which is the realistic case. Because the available positions in the lattice are finite, when either N or T grow, the probability to observe a unique bid progressively approaches zero [29].

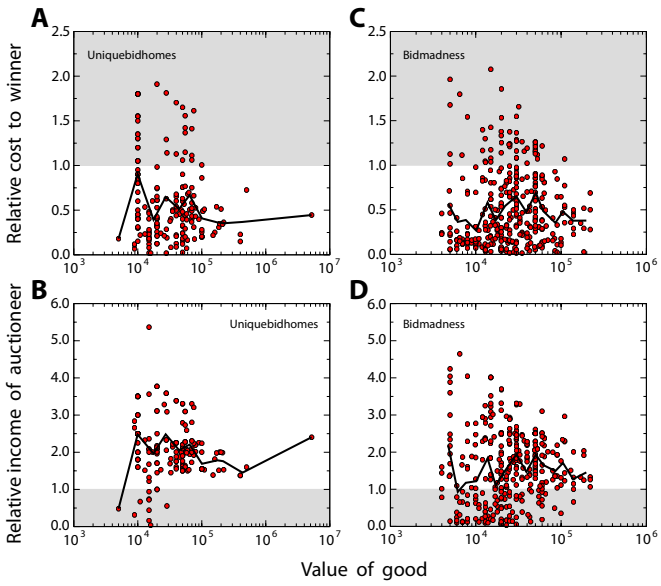

Figure 5: **Economic return of agents.** Auction winners tend to pay half of the value of the good, while auctioneers tend to earn twice the value of the good. We consider two different data sets, one regarding lowest unique bid auctions [`www.uniquebidhomes.com`, (A) and (C)] and the other highest unique bid auctions [`www.bidmadness.com.au`, (B) and (D)]. The unit is one hundredth of an Australian dollar. **(A)** Relation between the relative cost $(T_w\, c + b^*)\,/V$ to the winner of an auction and her income V. T_w indicates the number of bids made by the winner of the auction, c is the cost of the fee, b^* indicates the value of the winning bid, and V is the value of the good put up for auction. Each point represents an auction. The gray area corresponds to the region of negative return for winners of the auctions. The black line indicates the average value of the relative cost to the winners. Auctions are, on average, very profitable for the agent winning the auction, but the probability of a specific agent winning the auction is very low. Data refer to the data set `www.uniquebidhomes.com`. **(B)** Relative income $(B\, c + b^*)\,/V$ of the auctioneers as a function of their investment V. B is the number of bids placed by all agents. The gray area denotes the region of negative return for the auctioneers. The black line indicates the average value of the relative profit of the auctioneers. On average, organizing auctions is very profitable. Data refer to the data set `www.uniquebidhomes.com`. **(C)** Relation between the relative cost to the winner of an auction and her income for the data set `www.bidmadness.com.au`. **(D)** Relative income of the auctioneers as a function of their investment for the data set `www.bidmadness.com.au`.

Notice that at the saddle point $\gamma_s = \beta_s$, all $N+1$ agents are using the same bidding strategy and therefore they all have the same chances to win the auction. In particular, the probability that a generic agent wins the auction is $w_{\beta_s,\gamma_s} \leq 1/\,(N+1)$, where the inequality may arise because a unique and lowest bid may not exist.

The value of the exponent, corresponding to the optimal Lévy flight strategy in lowest unique bid auctions, is distinct from the one found in the case of purely random searches [10], and empirically observed in the movement patterns of foraging animals [1–8]. The quantitative difference arises, we believe, as a consequence of the anisotropy of the bid space (low values are favored), the role of competition, and, more importantly, the fact that the target is not "static" but moving according to the actions of the whole population of agents.

Discussion

In lowest unique bid auctions, agents have the possibility to win goods of high value for impossibly low prices (Figs. 5A and 5C), However, these all-pay auction markets are designed to be very profitable for the auctioneers [30–33], who, on average, double their investment (Figs. 5B, 5D and Supporting Information). For auctioneers, the profitability of lowest unique bid auctions is in fact guaranteed by the validity of the inequality $V < B\, c$, where B stands for the total number of bids and equals $(N+1)\, T$ in our model. Under this constraint however, the payoff of a generic agent in a perfectly rational population is always negative since

$$r_{\beta_s,\gamma_s} < w_{\beta_s,\gamma_s}\, V \leq \frac{V}{N+1} < T\, c \ ,$$

and there is no expected economic gain to be obtained for participating as a bidder in the auction markets. The rationality of the economic agents in adopting optimal strategies seems, therefore, in contrast with the ultimate irrationality that induces agents to take part in these auction markets.

Competitive irrationality, based on rational choices, has been investigated in economic theories [34–37], such as the dollar auction game [38]. The decision to participate or not participate in lowest unique bid auctions presents a paradox for potential bidders. If the number of agents participating in the auction is not too high, then the auction would bring a positive economic return to the agents, but not to the auctioneers. For example, in the case in which only one bidder participates in the auction, this bidder would have the maximal economic return by placing a single bid on the lowest value allowed. But by this token, every agent will feel that participating is profitable as long as not many other agents have bid yet. However, no agent can know how many other agents will actually bid on the good.

Our results raise a number of important research questions. First, which brain regions are responsible for implementing the search strategies used by agents? Since agents use similar search strategies to bees or birds, it is likely that there is no frontal cortex involvement. Using neuroimaging techniques such as fMRI it should be possible to answer this question. Second, does the economic paradox that the agents face reveal itself in brain activity patterns? Specifically, do some of the changes in brain activity observed for preference reversal [39, 40] occur also in this case? Additionally, our results suggest that controlled lowest unique bid auction markets would offer the possibility to run large-scale experiments at relatively low cost [41]. These experiments could be used for monitoring the behavior of agents in auction markets with tunable optimal

search strategies, and see if (and how fast) agents are able to adapt their behavior to optimality.

materials

Data have been collected from three publicly accessible web sites: www.uniquebidhomes.com, www.lowbids.com.au and www.bidmadness.com.au. Also, we make available a version of these data at the web page filrad.homelinux.org/resources.

Acknowledgments

We thank A. Arenas, A. Flammini, S. Fortunato, A. Lancichinetti, and J.J. Ramasco for useful discussions. T. Rietz is gratefully acknowledged for fundamental comments on the manuscript.

[1] G.M. Viswanathan *et al.*, *Nature* **381**, 413 (1996).
[2] F. Bartumeus *et al.*, *Proc. Natl. Acad. Sci. USA* **100**, 12771 (2003).
[3] G. Ramos-Fernández *et al.*, *Beahv. Ecol. Sociobiol.* **55**, 223 (2004).
[4] S. Bertrand, J.M. Burgos, F. Gerlotto, J. Atiquipa, *J. Mar. Sci.* **62**, 477–482 (2005).
[5] D.W. Sims *et al.*, *Nature* **451**, 1098 (2008).
[6] G.M. Viswanathan, E.P. Raposo, M.G.E. da Luz, *Phys. Life Rev.* **5**, 133 (2008).
[7] N.E. Humphries *et al.*, *Nature* **465**, 1066 (2010).
[8] G.M. Viswanathan, *Nature* **465**, 1018 (2010).
[9] M.F. Shlesinger, G.M. Zaslavsky, J. Klafter, *Nature* **363**, 31 (1993).
[10] G.M. Viswanathan *et al.*, *Nature* **401**, 911 (1999).
[11] D. Brockmann, L. Hufnagel, T. Geisel, *Nature* **439**, 462 (2006).
[12] R. Mantegna, H.E. Stanley, *Nature* **376**, 46 (1995).
[13] T.W. Malone, J. Yates, R.I. Benjamin, *Commun. ACM* **30**, 484 (1987).
[14] Y. Bakos, *Commun. ACM* **41**, 35 (1998).
[15] E. van Heck, P. Vervest, *Commun. ACM* **41**, 99 (1998).
[16] D. Lucking-Reiley, *J. Ind. Engineering* **48**, 227 (2000).
[17] M. Grieger, *Eur. J. Oper. Res.* **144**, 280 (2003).
[18] D. Lucking-Reiley, D. Bryan, N. Prasad, D. Reeves, *J. Ind. Engineering* **55**, 223 (2007).
[19] N. Augenblick, Unpublished manuscript available at www.stanford.edu/∼ned789 (2009).
[20] T. Hinnosaar, Unpublished manuscript available at toomas.hinnosaar.net/pennyauctions.pdf (2010).
[21] J.W. Byers, M. Mitzenmacher, G. Zervas, arXiv:1001.0592 (2010).
[22] S. Mittal, Unpublished manuscript available at www.stanford.edu/∼sonalm/Mittal_Penny_Auctions.pdf (2010).
[23] B.C. Platt, J. Price, H. Tappen, Unpublished manuscript available at econ.byu.edu/Faculty/Platt/Assets/PayToBid.pdf (2010).
[24] D.H. Hughes, M.F. Shlesinger, E.W. Montroll, *Proc. Natl. Acad. Sci. USA* **78**, 3287–3291 (1981).
[25] A. Clauset, C.R. Shalizi, M.E.J. Newman, SIAM Rev **51**, 661–703 (2009).
[26] J. Nash, *Proc. Natl. Acad. Sci. USA* **36**, 48 (1950).
[27] A. Rapoport, *N-person Game Theory: Concepts and Applications* (Univ. of Michigan Press, Ann Arbor, 1970).
[28] T. Başar, G.J. Olsder, *Dynamic Noncooperative Game Theory* (Academic Press, San Diego, 1995).
[29] G. Berkolaiko, S. Havlin, *Phys. Rev. E* **55**, 1395 (1997).
[30] R.B. Meyerson, *Math. Oper. Res.* **6**, 58 (1981).
[31] P.R. Milgrom, R.J. Weber, *Econometrica* **50**, 1089 (1982). .
[32] R.P. McAfee, J. McMillan, *Econ. Lett.* **23**, 343 (1987).
[33] V. Krishna, *Auction Theory* (Elsevier, New York, 2002).
[34] B.M. Staw, *Organ. Behav. Hum. Perf.* **16**, 27 (1976).
[35] B.M. Staw, J. Ross, *Science* **246**, 216 (1989).
[36] M.H. Bazerman, M.A. Neale, *Negotiating Rationally*. (Maxwell Macmillan International, New York, 1992).
[37] C. Wald, *Science* **322**, 1624 (2008).
[38] M. Shubik, *J. Conflict Resolut.* **15**, 109 (1971).
[39] D.M. Grether, C.R. Plott, *Am. Econ. Rev.* **69**, 623 (1979).
[40] A. Tversky, P. Slovic, D. Kahneman, *Am. Econ. Rev.* **80**, 204 (1990).
[41] M.J. Salganik, P.S. Dodds, D.J. Watts, *Science* **311**, 854 (2006).

S 1. "LOWEST UNIQUE BID" AND "HIGHEST UNIQUE BID" AUCTIONS

A. Description of the auction

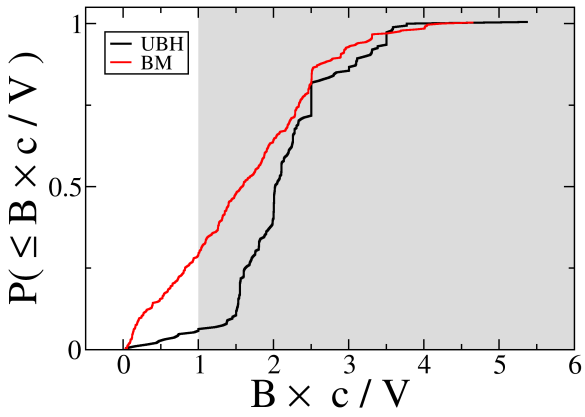

Figure S1: Cumulative distribution of the relative return $(B \times c)/V$ for the auctioneers. For `www.uniquebidhomes.com` data set (black line) the 95% of the auctions are in the gray region of positive return, where the relative return $(B \times c)/V > 1$. On average, the relative return of the auctioneers is 2.2. For `www.bidmadness.com.au` data set (red line) the 72% of the auctions have produced a positive relative return and on average the relative return is 1.6.

Lowest Unique Bid (LUB) auctions are special on-line auctions which have reached a considerable success during last years. Their peculiarity consists in the fact that they are reverse auctions: rather than the bidder with the highest bid (as in the case of traditional auctions), the winner is the person who makes the LUB (see Figure 1a in the main text). The rules of a LUB auction are very simple. At the beginning of each auction, the auctioneers put up for auction a good of value V. After the beginning of the auction and for a certain period of time (in general of order of weeks), agents participate to the auction by making bids. The natural unit of the auction is one hundredth of dollars, euros, etc (i.e., the currency depends on the country where the auction is hosted). Bids may be any amount (in cents) between one cent and a maximal bid amount M (generally lower than ten hundreds of cents). Sometimes, the value of M is not fixed, but the bid space is anyway naturally bounded since none of the agents wants to bid more than V. The value of V depends on the auction, but generally its order of magnitude is of thousands of hundreds of cents. Making a bid costs a fee c (typically from one hundred to ten hundreds cents). After each bid b, the agent receives an automatic message, from the web site hosting the auction, saying whether that bid was the winning bid (i.e., the bid is the LUB) or not. The agent is constantly informed about the status of her bids (i.e., whether one of them becomes the LUB or is not longer the LUB). However, each agent knows only what she has bid, without any information on which values the other agents have bid. In general, there is no restriction for the number of bids that the same agent may place. When the time dedicated to the auction expires, the winner is the agent who made the LUB and can therefore purchase the good for the value of her winning bid. If at the close of the auction a single lowest unique bid does not exist, the successful bid becomes the lowest one made by only two agents and the winner is the one who has bid first on such value. In the case in which also a bid made by only two agents does not exists, then the winning bid becomes the lowest one made by only three agents and so on. Again in these situations, the winner is the agent who has first placed a bid on the winning value. In our data sets however, we always observe that the winning bid is an unmatched bid.

There are several slight variations of this kind of auctions. Very often, the end of the auction is not determined by an expiration time, but by a minimum required number of bids, *a priori* fixed by the auctioneers. In other variations called Highest Unique Bid (HUB) auctions, the winning bid is the unique one closest to M.

Independently on the type of auctions, this kind of auctions are particularly profitable for both the auctioneers and the winners of the auctions. Figure 5 of the main text and Figure S1 clearly show that there are only few exceptions in which auctioneers or winners have lost money, but in the majority of the auctions their returns are positive.

Data set	Tot. Auctions	Tot. Agents	Tot. Bids	$\langle M \rangle$	$\langle c \rangle$	$\langle N \rangle$	$\langle B \rangle$
UBH	189	3 740	55 041	362	437	50	6
LB	55	445	3 740	1 284	478	13	6
BM	336	3 719	127 275	504	174	40	14

Table S1: Summary table of the data sets analyzed in this paper. We report, from left to right, the name of the data set, the total number of auctions, the total number of different agents, the total number of bids, the average value of the maximal bid value, the average amount of the fee, the average number of agents involved in an auction and the average number of bids made by a single agent in a single auction. The unit of the bid values is one hundredth of an Australian dollar.

B. Description of the data sets

We collected data from the web sites `www.uniquebidhomes.com` (UBH), `www.lowbids.com.au` (LB) both hosting LUB auctions and from `www.bidmadness.com.au` (BM) organizing HUB auctions. Data regard all auctions organized during 2007, 2008, 2009 and part of 2010 by these web sites. We collected detailed information concerning the auctions: the value of the goods, the cost of the fee, the maximum bid amount, the duration of the auction or eventually the required number of bids. We report in Table S1 some of these quantities calculated for our data sets. We were able also to keep track, for all data sets, of each single bid, getting information about its value, the time when it was made and the agent who made it. Data sets were anonymised and can be downloaded at the page `filrad.homelinux.org`. In the following, we focus our analysis mainly on the data sets UBH and BM since, given their size, allow to perform much better statistics.

C. Analysis

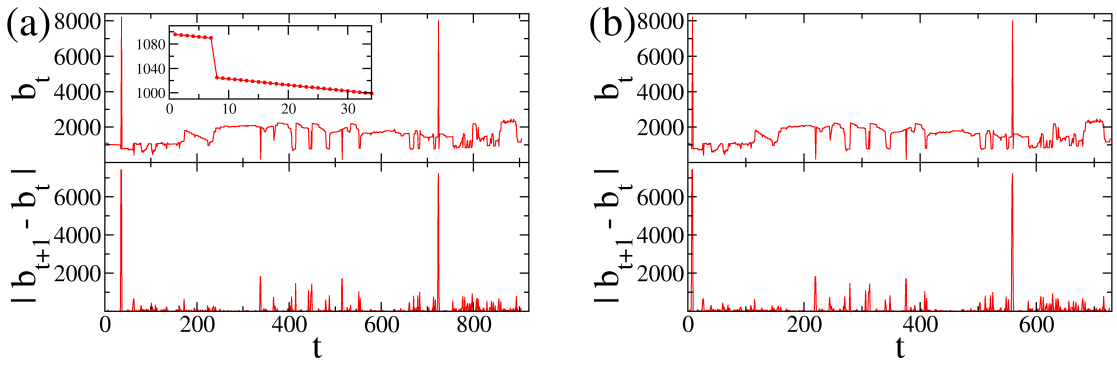

Figure S2: UBH data set. (a) In the top panel, the time series of bid values performed by agent $u = 1632$ in auction $a = 19$ is shown. In particular we zoom into a region where "abnormal" movements are present. In the bottom panel, we plot the time series of the length of her jumps $d_t = |b_{t+1} - b_t|$. (b) Same plots as those appearing in panel a, but for the cleaned version of the time series. The indices a and u refer to the anonymised version of the UBH data set.

Fixed an auction a and an agent u, we consider the temporal series of her bids, whose total number is denoted by $T_{a,u}$. This series is basically a list of integers $b_1, b_2, \ldots, b_T$, where we have suppressed the indices a and u for shortness of notation. Their value is defined over the interval $[1, M]$. All bs are different each other since no agent bids on a certain value more than once. A typical example of these time series is reported in the top panel of Figure S2a. We calculate the gap or difference between subsequent bid values and indicate it with $d_t = |b_{t+1} - b_t|$. Given a list of T bid values we can in fact extract a list of $T - 1$ differences between consecutive bids. In the bottom panel of Figure S2a, we plot the time series d_t for the same agent whose bid time series is plotted in the upper panel.

D. Cleaning the data sets

Generally, more "professional" agents perform random searches followed by systematic coverages of intervals. A typical example is shown in the inset of the upper panel of Figure S2a. Here a zoom of the time series appearing in the main plot is reported. Systematic coverages are performed by selecting a range of bid values and then placing a bid on each single value in that interval. This is an opportunity offered by the web site hosting auctions. Each bid in this case is characterized by the same time stamp. Such occurrence is likely for agents who make a significant number of bids, but becomes less relevant for agents who invest relatively small amount of money. We cleaned data by removing all pieces of the time series corresponding to this "abnormal" behavior. It should be remarked that the gaps between consecutive bids which can be measured in these regions are in the majority of the cases equal to one. Including these regions will influence only gaps equal to unity by overestimating their presence. We decided to remove such systematic coverages in order to focus our attention only on "normal" bidding strategies. The result, after the cleaning procedure of time series shown in Figure S2a, is reported in the upper panel of Figure S2b. The gaps between consecutive bids in the cleaned time series are reported in the bottom panel of Figure S2b.

As additional information, in Figure S3, we measure the number of agents $N(\rho)$ performing a ratio ρ of bids made using a

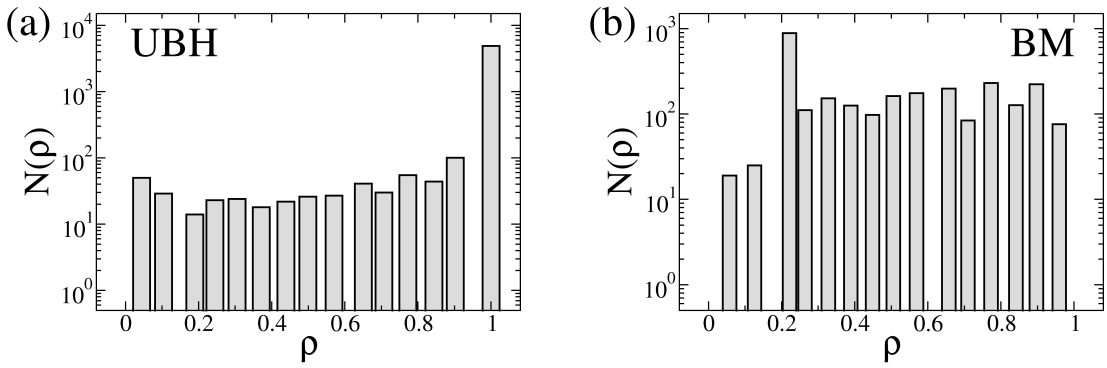

Figure S3: Number of agents $N(\rho)$ performing "normal" search strategies at rate ρ.

normal strategy (i.e., after removing systematic coverages) and the total number of bids placed.
In the following analysis, we consider only cleaned time series, where systematic coverages have been deleted.

E. Statistics of the length of the jumps

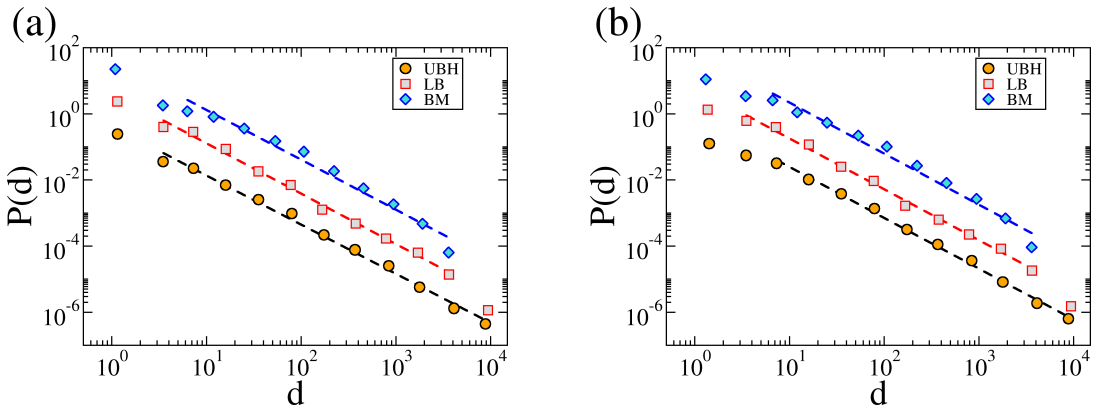

Figure S4: (a) Probability distribution function $P(d)$ calculated over all agents and auctions in the data sets UBH (orange circles), LB (gray squares) and BM (turquoise diamonds). Dashed lines stand for best power-law fits (least square). We find $\alpha = 1.54(2)$ [black], $\alpha = 1.54(3)$ [red] and $\alpha = 1.54(5)$ [blue]. (b) Same as in panel a, but for cleaned time series. Dashed lines have slopes $\alpha = 1.49(2)$ [black], $\alpha = 1.52(2)$ [red] and $\alpha = 1.51(5)$ [blue]. The data of this figure also reported in Figure 3A of the main text. Curves calculated for LB and BM data sets have been vertically shifted for clarity.

We measure the probability distribution function (pdf) $P(d)$ of the difference between subsequent bids made by single agents in single auctions. Global (i.e., aggregated over all agents and auctions) pdfs of both data sets are plotted in Figure S4. For agents with a sufficient number of bids in the same auction, we also compute individual pdfs. Some examples are reported in the various panels of Figures S5, S6 and S7 for UBH data set and in Figures S8, S9 and S10 for BM data set. In each panel of these figures, we explicitly indicate the id of the auction a and the id of the agent u as they appear in our anonymised version of the data sets. In all cases, we find a behavior compatible with

$$P(d) \sim d^{-\alpha} \quad . \tag{S1}$$

The search strategy adopted by agents is therefore given by Lévy flights with characteristic exponent α. The best fits with power-laws are plotted in Figures S5, S6, S7, S8, S9 and S10 with black dashed lines and the value of α, plus the associated error, corresponding to the best fit is reported at the top of each panel.
In order to calculate a pdf, we divide the range of possible values of d in bins equally spaced on the logarithmic scale. We then drawn the pdf by associating to each bin the number of ds falling in that bin divided by the number of integers that could enter in the bin (this because d can assume only integer values). Everything is then normalized by simply dividing by the total number of points. We compute the best power-law exponent by performing a linear least square fit in double logarithmic scale. Despite the binning procedure may introduce a certain amount of arbitrariness in the evaluation of the pdfs, we checked the consistency of our results by varying the number of bins. Moreover, we additionally make use of a different fit method (maximum likelihood) about which we will discuss later.

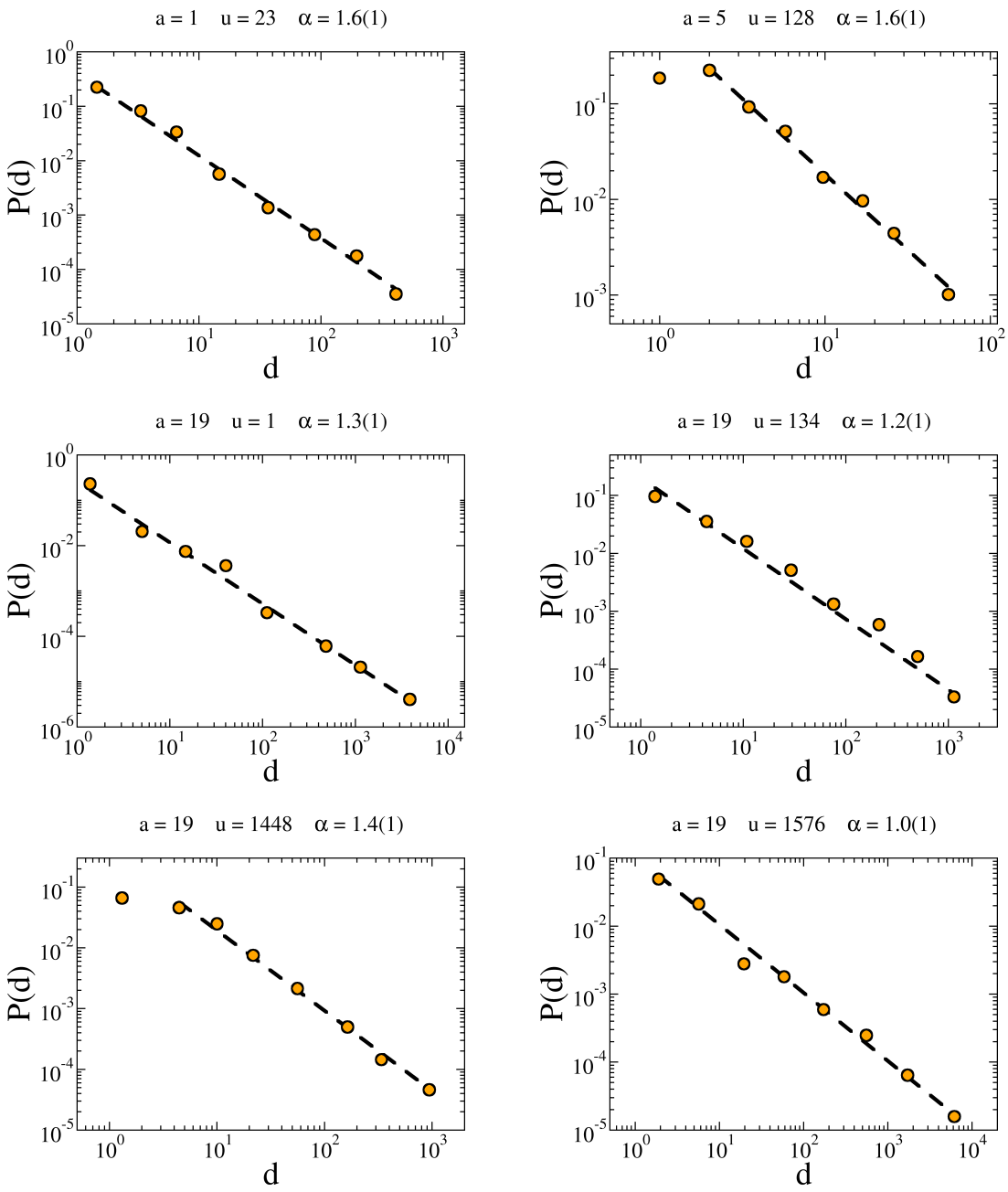

Figure S5: UBH data set. Probability distribution function $P(d)$ measured for agent u in auction a. We show several $P(d)$s for different pairs u and a. Dashed lines denote the best power-law fit (least square) $P(d) \sim d^{-\alpha}$ obtained for the data.

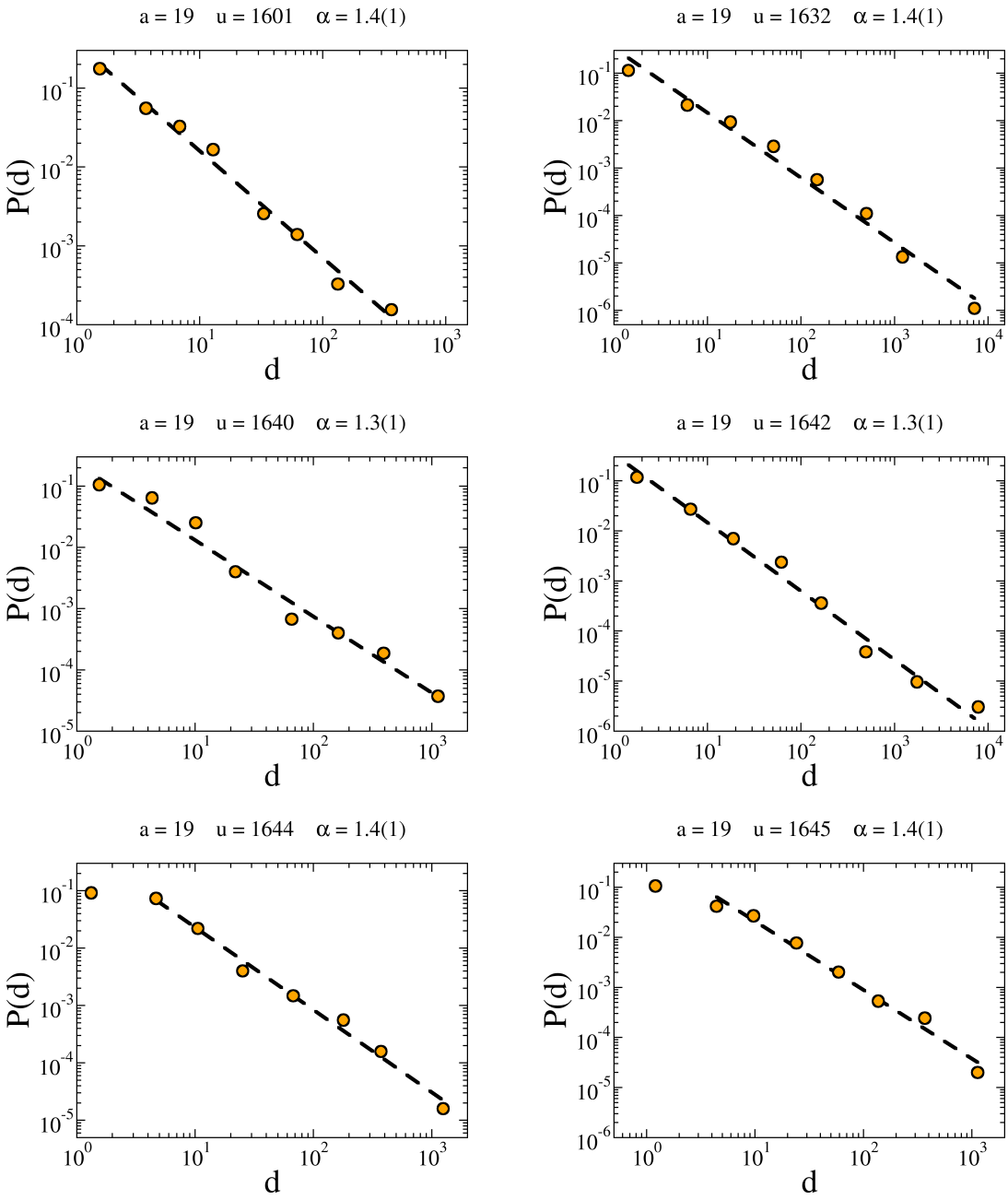

Figure S6: UBH data set. Same as Figure S5.

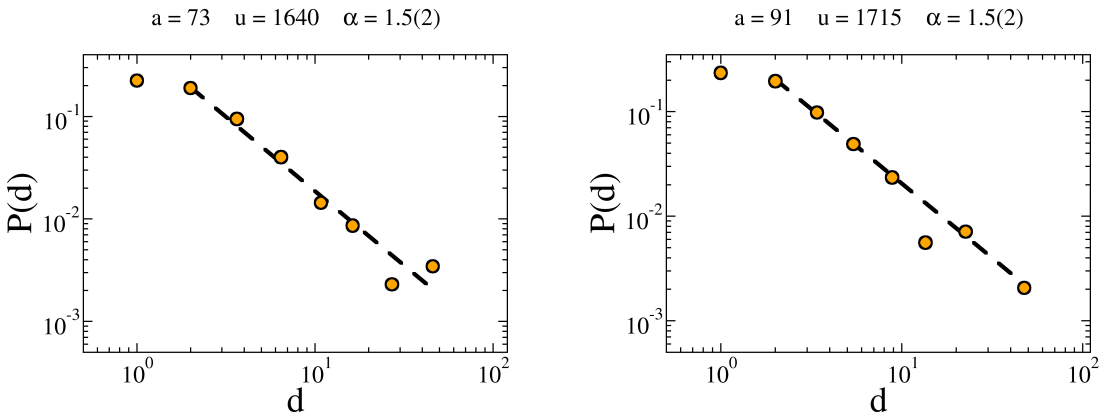

Figure S7: UBH data set. Same as Figure S5 and S6.

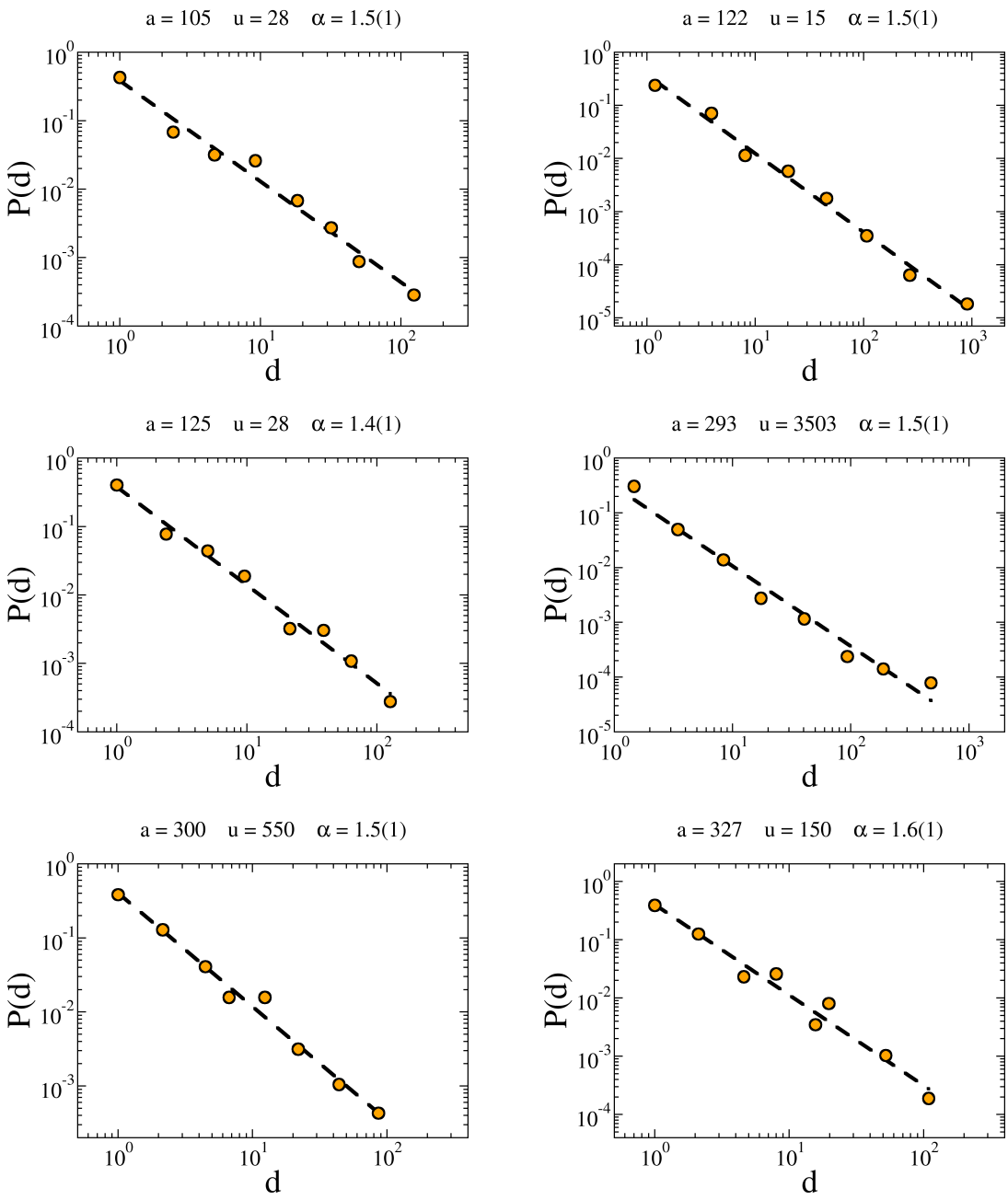

Figure S8: BM data set. Probability distribution function $P(d)$ measured for agent u in auction a. We show several $P(d)$s for different pairs u and a.

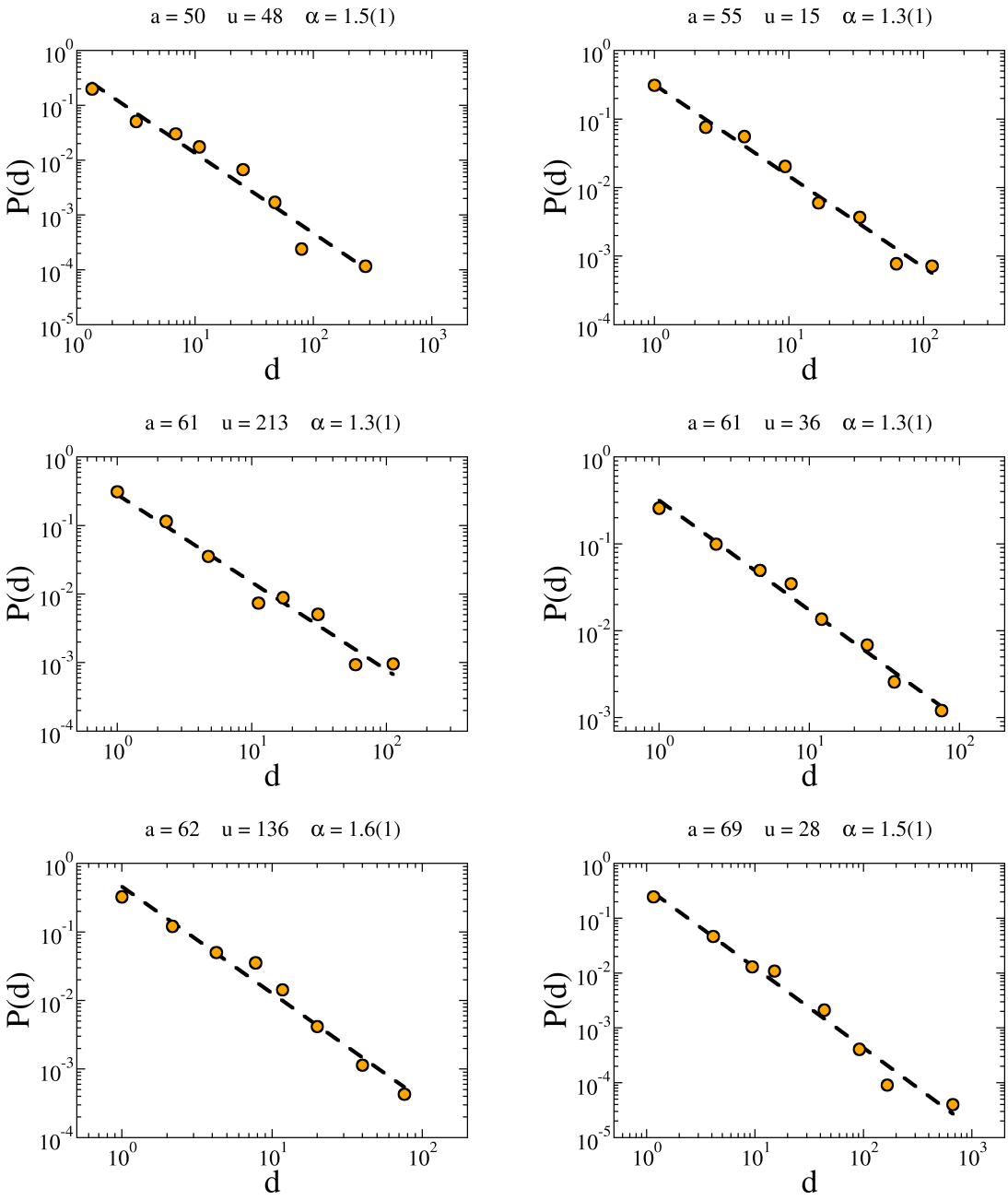

Figure S9: BM data set. Same as Figure S8.

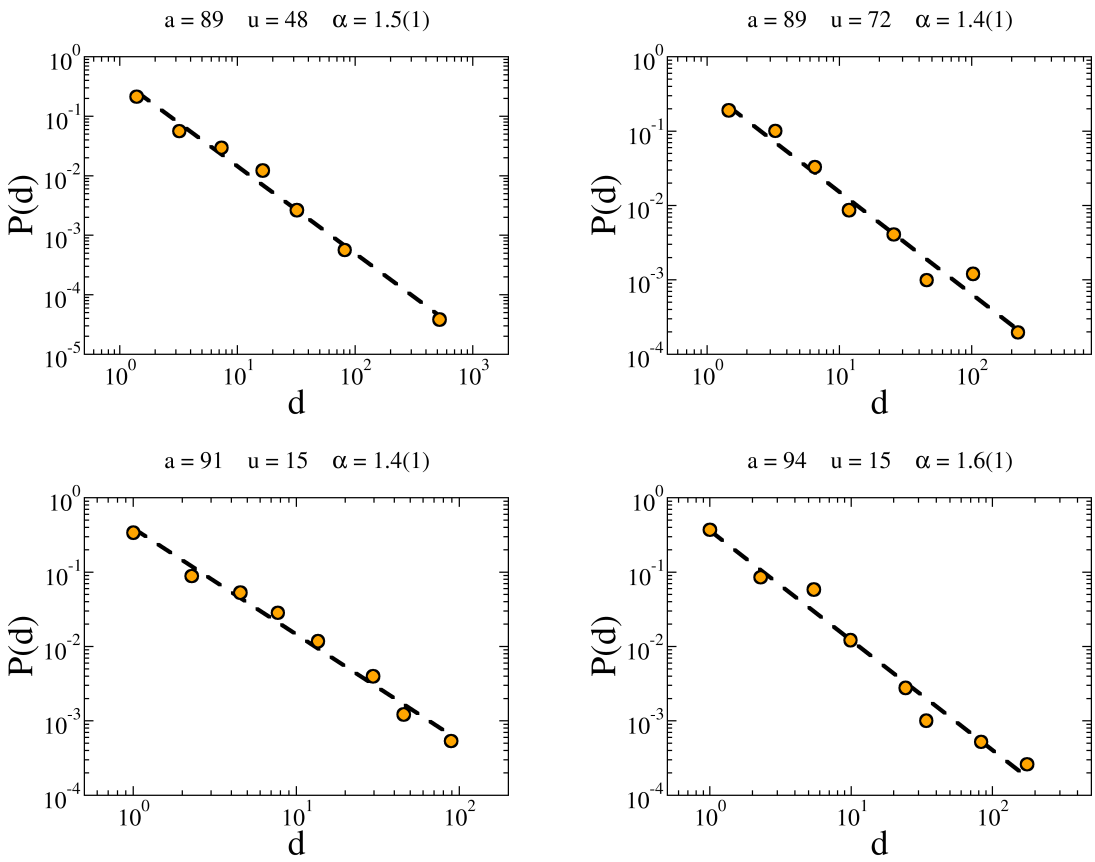

Figure S10: BM data set. Same as Figure S8 and S9.

F. Independence of the direction of the jumps

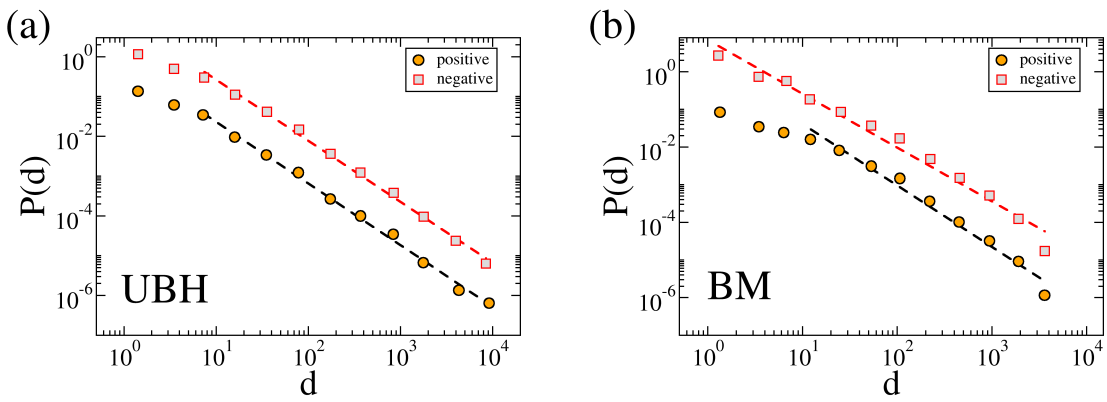

Figure S11: (a) UBH data set. Probability distribution function $P(d)$ calculated over all agents and auctions. We have separated positive from negative variations. The measured decay exponents of the best fits with power-laws (dashed lines) are $\alpha = 1.53(2)$ [black] and $\alpha = 1.54(2)$ [red], respectively. The curve corresponding to negative variation has been vertically shifted for clarity. This figure appears also in Fig. 3B of the main text. (b) BM data set. here the best power-law fit are $\alpha = 1.61(8)$ [black] and $\alpha = 1.45(4)$ [red].

Since the rules of the auction naturally bring agents to move towards low bid values, it is important to stress any eventual difference between the statistics associated with the length of gaps between consecutive bid values. We aggregated data from all agents and auctions and separate positive (i.e., $b_{t+1} > b_t$) from negative (i.e., $b_{t+1} < b_t$) variations. In Figure S11 the pdfs of positive and negative variations are plotted together. As one may notice, there is not a significant difference between them and both show a clear power-law decay with compatible exponents.

G. Independence of the agents' activity

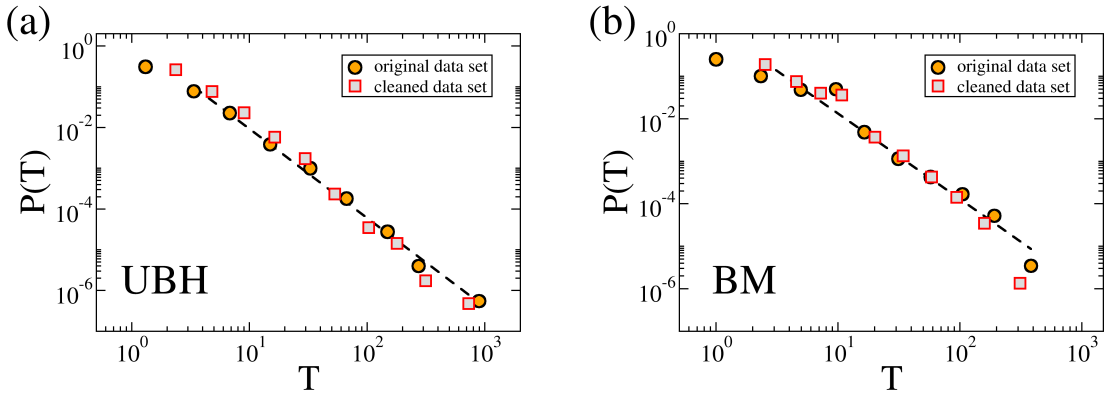

Figure S12: (a) UBH data set. Probability distribution function $P(T)$ of the number of bids T performed by single agents in single auctions. We calculate $P(T)$ on the original data set (orange circles) and on the cleaned version of the same data set (gray squares). In both cases, the distribution scales power-like with a decay exponent equal to $2.2(2)$. (b) BM data set. The exponent of the best fit is $2.0(4)$ [dashed line].

The evidence of Lévy flights for single agents in single auctions can be directly verified only for agents with a sufficient number of bids T in the same auction. For values of T smaller than 50 is practically impossible to construct the histogram $P(d)$ and therefore no exponent can be measured. Unfortunately, this situation is very frequent in our data sets. We measure the number of bids made each agent in each auction and plot the pdf of the number of bids in a single auction in Figure S12. The level of activity is quite heterogeneous and decays power-like with an exponent close to 2.2. For completeness, we measure the same pdf for both original and cleaned data sets without noticing appreciable differences.

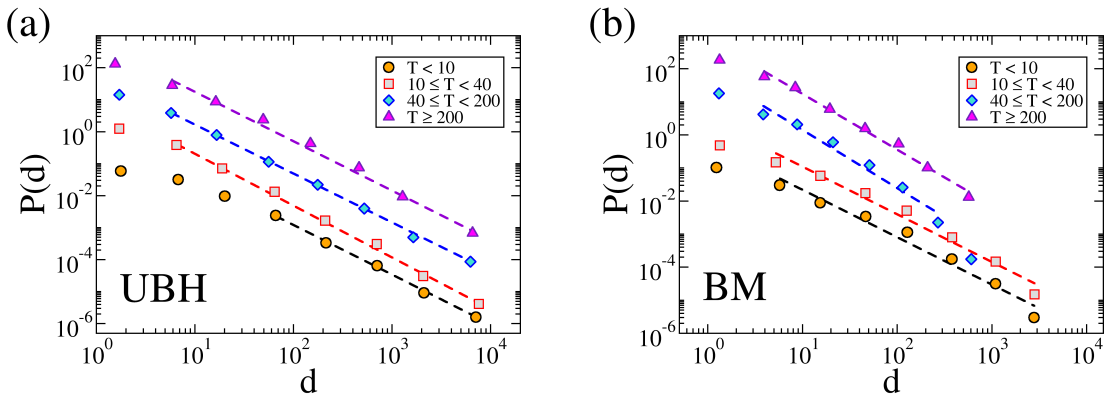

Figure S13: (a) UBH data set. Probability distribution function $P(d)$ of the length d of the jumps performed by agents in the bid space. All auctions have been aggregated together. Different curves correspond to agents with different levels of activity. Their activity is measured as the number of bids made in the same auction. We divide the population into four subsets: $T < 10$ (orange circles), $10 \leq T < 40$ (gray squares), $40 \leq T < 200$ (blue diamonds) and $T \geq 200$ (violet triangles). Dashed lines represent the best power-law fits. The value of the measured exponents are: $\alpha = 1.55(2)$ (black), $\alpha = 1.62(4)$ (red), $\alpha = 1.53(2)$ (blue) and $\alpha = 1.54(3)$ (violet). Curves have been vertically shifted for clarity. This figure is also reported in Fig. 3C of the main text. (b) BM data set. Best power-law fits (dashed lines) have exponents: $\alpha = 1.43(4)$ (black), $\alpha = 1.44(5)$ (red), $\alpha = 1.7(1)$ (blue) and $\alpha = 1.7(1)$ (violet).

We divide the population in different ranges of activity. We aggregate the length of the jumps performed by all agents in a given

bin and measure the resulting $P(d)$. The results of this analysis are reported in Figure S13. Independently of the activity level, the aggregated pdfs decay power-like and have similar exponents α. This means that the presence of Lévy flights is typical for every agent independently of how many bids the agent has made.

H. Independence of the bidding time

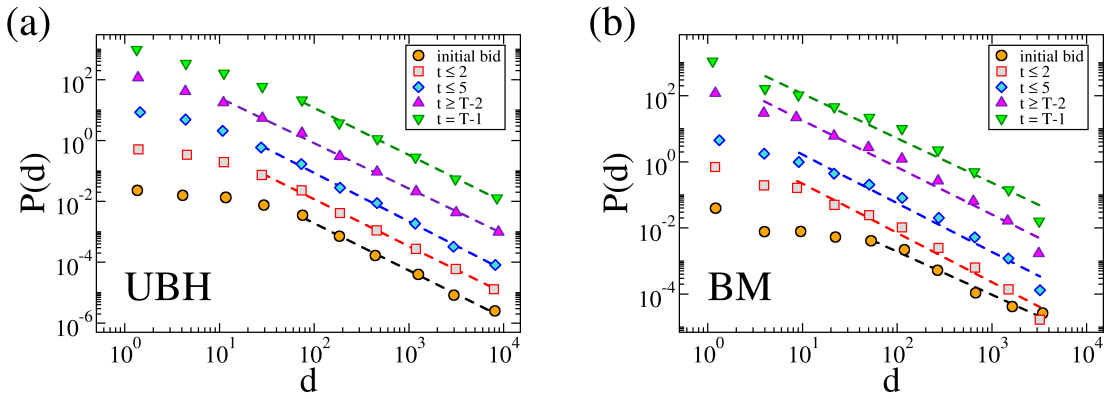

Figure S14: (a) UBH data set. Probability distribution function $P(d)$ of the length d of the flights performed by agents in the bid space. All auctions have been aggregated together. Different curves correspond to different periods of activity for agents: orange circles correspond to the initial guess made by agents; bids gaps with $t \leq 2$ (gray squares) and $t \leq 5$ (blue diamonds) aggregate the data corresponding to the early activity of agents; $t \geq T-2$ (violet up triangles) and $t = T-1$ (green down triangles) corresponds to the jumps made by agents at the end of their own activity. Dashed lines have been obtained as best power-law fits with data points. The value of the measured exponents are: $\alpha = 1.55(4)$ (black), $\alpha = 1.54(3)$ (red), $\alpha = 1.59(4)$ (blue), $\alpha = 1.49(5)$ (violet) and $\alpha = 1.54(6)$ (green). Curves have been vertically shifted for clarity. This figure is also reported in Fig. 2d of the main text. (b) BM data set. Best power-law fits (dashed lines) have exponents: $\alpha = 1.3(1)$ (black), $\alpha = 1.50(5)$ (red), $\alpha = 1.47(4)$ (blue), $\alpha = 1.43(6)$ (violet) and $\alpha = 1.35(6)$ (green). For the initial bid b_1, we compute the length of the jump as $d = M - b_1 + 1$, with M being the maximal bid value in the HUB auctions.

Another fundamental point is to understand whether the Lévy flight strategy is emergent or *a priori* given. We test these hypotheses by measuring the pdfs $P(d)$ corresponding to a certain range during the activity of the agents. The results are reported in Figure S14. We consider ranges of activity periods corresponding to $t \leq 2$, $t \leq 5$, $t \geq T-2$ and $t = T-1$. Additionally, we consider the distribution of the initial bid values (i.e., the first bid made by all agents in all auctions). In every case, we are able to fit the curves with power-laws and the resulting exponents are compatible each other. We can effectively conclude that the strategy to adopt a Lévy flight is not an emergent property induced by the evolution of the auction. Instead the strategy to follow Lévy flights is intrinsically present, in each agent, during the whole duration of the auction.

I. Independence between jumps

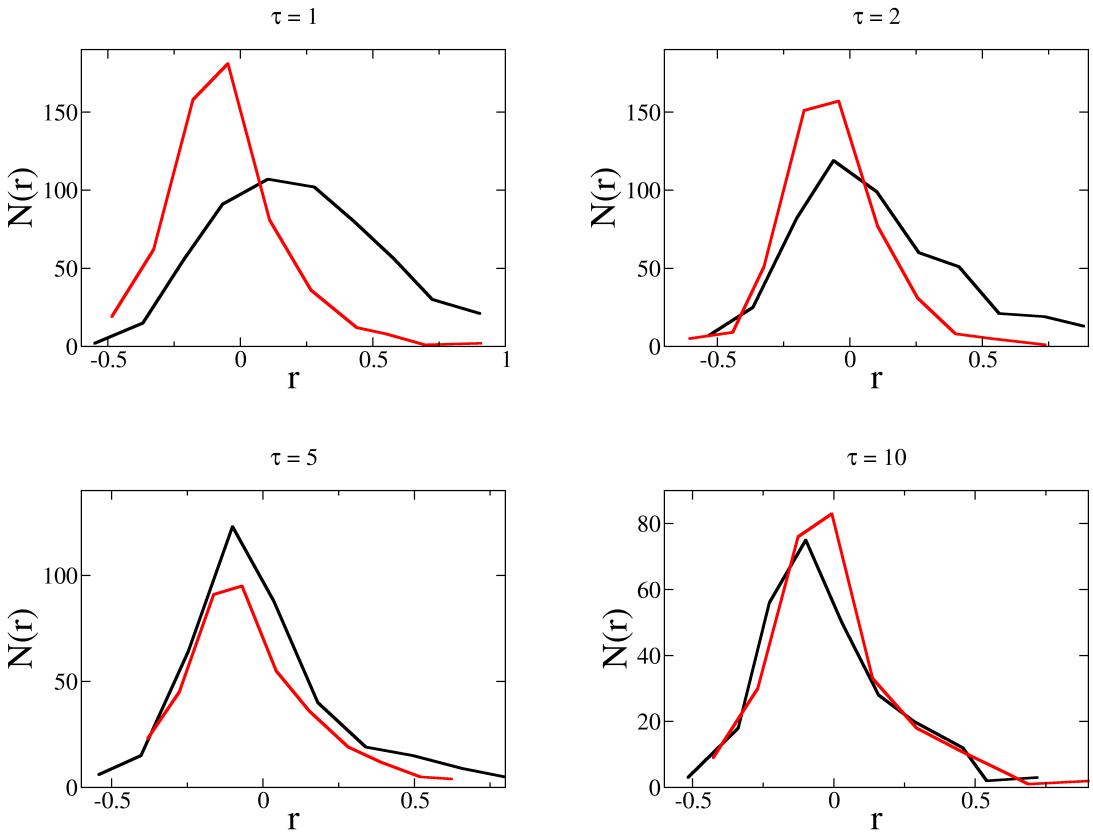

Figure S15: UBH data set. Number of agents $N(r)$ whose bid gaps at position t and $t+\tau$ have Pearson's correlation coefficient equal to r. Black curves are measured on real data, while the red ones are calculated over a reshuffled version of the same data. The reshuffling is made by randomly exchange pairs of entries in the time series of the time gaps with the only prescription that the sum of them is not lower than one and not larger than M. We consider different values of τ. In each plot only agents with at least $10+\tau$ bids in the same auction are considered.

We further study the correlations between jumps. Given an agent and an auction, we consider the list of all her jumps $d_1, d_2, \ldots, d_{B-1}$ and calculate the Pearson's correlation coefficient

$$r_\tau = \frac{\langle (d_t - \mu_t)\,(d_{t+\tau} - \mu_{t+\tau})\rangle}{\sigma_t\,\sigma_{t+\tau}} \quad , \tag{S2}$$

where $\langle\cdot\rangle$ stands for the average over the entire time series (i.e., over all values of t from 1 to $T-1-\tau$). $\mu_t = \langle d_t\rangle$ and $\mu_{t+\tau} = \langle d_{t+\tau}\rangle$ are the average values of the bid gaps along the time series, while $\sigma_t = \sqrt{\langle d_t^2\rangle - \langle d_t\rangle}$ and $\sigma_{t+\tau} = \sqrt{\langle d_{t+\tau}^2\rangle - \langle d_{t+\tau}\rangle}$ are the respective standard deviations. We measure such coefficient for every agent who has performed at least $10+\tau$ bids in the same auction and show the number of agents $N(r)$ with given value of r in Figures S15 and S16. The same quantity is also calculated for a randomized version of the time series, where bid gaps are randomly reshuffled with the only constraint that their partial sum cannot never be smaller than one and larger than M. We consider several values of τ. As one can clearly notice, subsequent gaps (i.e., $\tau = 1$) are slightly correlated. Such correlation, becomes negligible when τ grows and already for $\tau = 2$, $N(r)$ is negligible. For $\tau = 5$ and $\tau = 10$, the curves corresponding to the original time series and those obtained over randomly reshuffled time series are almost identical.

Such results show that agents perform almost uncorrelated Lévy flights. Once an agent makes a jump, the length of this jump is slightly correlated with the one of the jump made before. However, after few jumps there is not longer memory of what happened before. In good approximation, the walk of the agent in the bid space can be therefore modeled as the one followed

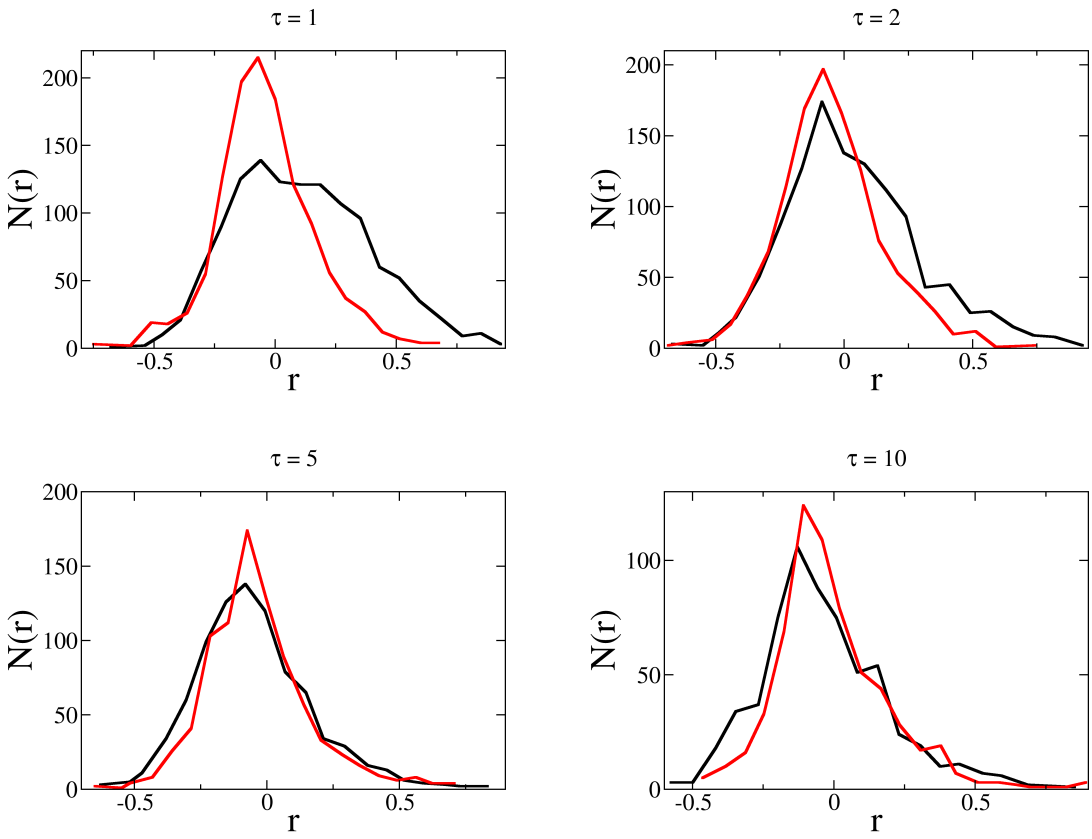

Figure S16: Same as those appearing in Figure S15 but for BM data set.

by a random walker performing uncorrelated Lévy flights.

J. Testing the model

1. Maximum likelihood fit and Goodness of fit

In this section, we compute the level of significance of our model for the description of real time series. Suppose that a time series of T bid values $b_1, b_2, \ldots, b_T$ describes a realization of our model. Fixed the exponent α, the bound M of the lattice and the position b_{t-1} at stage $t-1$, the probability that the random walker jumps at b_t at stage t is given by the transition matrix of Eq. (6) of the main text. The probability or *likelihood* that the whole sequence was extracted from our model is

$$p\left(b_1, b_2, \ldots, b_T \,|\alpha\right) = \left(Q_\alpha\right)_{0,b_1} \, \left(Q_\alpha\right)_{b_1,b_2} \, \left(Q_\alpha\right)_{b_2,b_3} \, \cdots \, \left(Q_\alpha\right)_{b_{T-1},b_T} \ .$$

The value of α that maximizes the former equation represents the most likely exponent of our model that could have generated our particular sequence. In order to find its maximum, it is convenient to take the logarithm of both sides and write the log-likelihood

$$\mathcal{L}\left(b_1, b_2, \ldots, b_T \,|\alpha\right) = \sum_{t=1}^{T} \ln\left[\left(Q_\alpha\right)_{b_{t-1},b_t}\right] = -\alpha \sum_{t=1}^{T} \ln|b_t - b_{t-1}| - \sum_{t=1}^{T} \ln\left[m_{b_{t-1}}\left(\alpha\right)\right] \ , \tag{S3}$$

where we set $b_0 = 0$. The value α' at which the maximum of Eq. (S3) occurs can be estimated numerically.
α' is the best exponent fitting the data in the hypothesis that they were produced according to our model. The significance level of the model for the description of the data can be calculated by estimating the p-value associated with our measurement. In this respect, we first compute the distance between the theoretical distribution of the jump lengths

$$P_{\alpha'}\left(d\right) = \left[\sum_{i,j} \left(Q_{\alpha'}\right)_{ij} \delta\left(d - |i-j|\right)\right] \left[\sum_{d} \sum_{i,j} \left(Q_{\alpha'}\right)_{ij} \delta\left(d - |i-j|\right)\right]^{-1}$$

and the one obtained from our data $P\left(d\right)$ by calculating

$$\eta_{data} = \max_t \left|P_{\alpha'}\left(\geq d_t\right) - P\left(\geq d_t\right)\right| \ ,$$

where $P\left(\geq d\right) = \sum_{q \geq d} P\left(q\right)$ is the cumulative distribution of the jump lengths. Notice that the distance between cumulative distributions is the same as the one adopted in the Kolmogorov-Smirnov test. We then generate artificial time series of length T from our model with exponent α' and compute their distance η with respect to the theoretical distribution. The p-value is finally determined by the relative number of times in which we observe $\eta \geq \eta_{data}$.
Synthetic time series generated according to our model can be additionally used for the determination of the error associated to the estimation of α'. The error associated to α' is the standard deviation of the best exponents estimated, with maximum likelihood, for the synthetic data sets.
A graphical comparison between the exponents α (least square method) and α' (maximum likelihood method) is presented in Figure S17. In general, the two methods produce consistent results. For completeness, we list the results obtained in Tables S2 and S3.

The p-values show also a general goodness of our model for the description of the data. Sometimes however, the value of p is very small. This could be explained in a simple manner. In Figure S18 we plot for example the statistical test performed over the same time series appearing in Figure S2. In that auction, the maximum bid amount was $M = 13\,000$. However, this value of M does not correspond to the "effective" bound felt by the agent. This bound seems to be around $M \sim 2\,000$ as the sudden drop of $P\left(\geq d\right)$ would suggest. By setting $M = 2\,200$ and running again the statistical test, as we did in Figure S18b, we see clearly that the curve predicted by our model and the one measured on real data are in very good agreement.

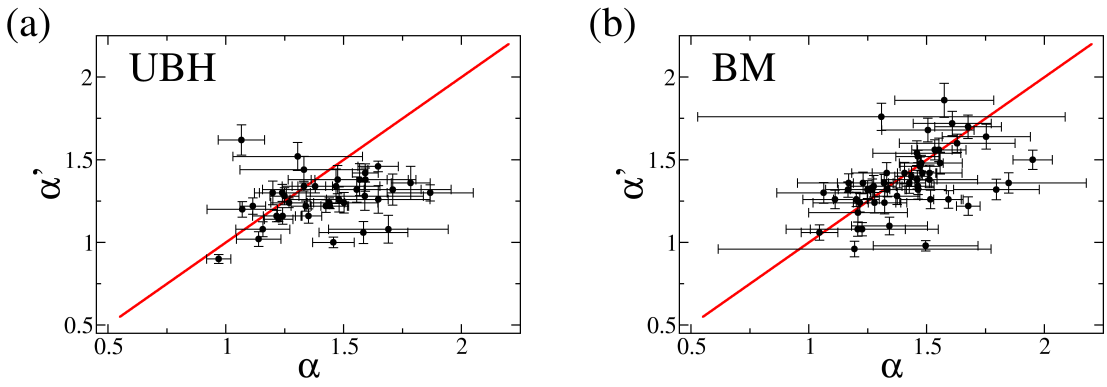

Figure S17: We consider only agents who have performed at least $T = 50$ bids in a single auction in UBH data set and those with at least $T = 100$ in the BM data set. Our data set offers 39 agents that satisfy this constraint in the UBH data set and 52 in the BM data set. Panels a (UBH) and b (BM) show the scatter plot α' *versus* α for the best power-law exponents estimated by using maximum likelihood and least square methods, respectively. The agreement between the two measurements is good as demonstrated by the fact that the majority of the points fall on the diagonal (red line).

a	u	α	α'	p
1*	23	1.6(1)	1.5(1)	0.00
1	81	1.2(1)	1.3(1)	0.17
100	1715	1.6(2)	1.1(1)	0.01
100*	81	1.5(2)	1.3(1)	0.00
104	3093	1.7(3)	1.1(1)	0.14
108	134	1.7(1)	1.3(1)	0.02
14	134	1.2(1)	1.1(1)	0.03
14*	81	1.9(2)	1.3(1)	0.00
15	423	1.6(4)	1.3(1)	0.3
179	3663	1.8(1)	1.4(1)	0.17
19	1	1.3(1)	1.3(1)	0.28
19	1313	1.2(1)	1.2(1)	0.14
19*	134	1.2(1)	1.1(1)	0.00
19	1433	1.1(1)	1.0(1)	0.06
19	1448	1.4(1)	1.2(1)	0.01
19	1558	1.1(1)	1.2(1)	0.63
19	1576	1.0(1)	0.9(1)	0.35
19	1601	1.4(1)	1.3(1)	0.01
19	1632	1.4(1)	1.2(1)	0.01
19*	1640	1.3(1)	1.2(1)	0.00
19	1642	1.3(1)	1.2(1)	0.13
19*	1644	1.4(1)	1.2(1)	0.00
19*	1645	1.4(1)	1.2(1)	0.00
19	3	1.2(1)	1.3(1)	0.9
19	363	1.2(1)	1.1(1)	0.02
19	434	1.1(1)	1.2(1)	0.35
19	438	1.5(1)	1.0(1)	0.02
20	617	1.6(2)	1.4(1)	0.01
22	134	1.2(1)	1.3(1)	0.95
44	433	1.1(1)	1.6(1)	0.07
46	2003	1.3(3)	1.5(1)	0.02
5*	128	1.6(1)	1.4(1)	0.00
62	2392	1.3(3)	1.4(1)	0.43
71*	324	1.6(2)	1.4(1)	0.00
73	1640	1.5(2)	1.4(1)	0.18
73	1715	1.5(1)	1.2(1)	0.34
79	134	1.6(2)	1.3(1)	0.11
91	1715	1.5(2)	1.3(1)	0.32
97	1715	1.6(2)	1.3(1)	0.09

Table S2: UBH data set. Each row corresponds to one of the 39 agents who have bid at least 50 times in the same auction. We report the id of the auction a, the id of the agent u, the exponent α calculated with the least square method, the exponent α' calculated with the maximum likelihood method and the p-value. Entries with low p-values are marked with *. In the 77% of the cases we find a p-value larger than 0, which indicates that our model well describe the time series.

a	u	α	α'	p
11	28	1.1(2)	1.3(1)	0.09
13*	48	1.5(1)	1.3(1)	0
13	28	1.3(1)	1.4(1)	0.04
15	11	1.8(3)	1.4(1)	0.05
15	36	2.0(1)	1.5(1)	0.03
28	28	1.4(1)	1.4(1)	0.58
32*	150	1.2(6)	1.0(1)	0
39*	48	1.3(1)	1.3(1)	0
47	28	1.1(1)	1.3(1)	0.48
50	48	1.5(1)	1.3(1)	0.27
52	28	1.2(2)	1.4(1)	0.01
55	15	1.3(1)	1.3(1)	0.38
55*	150	1.2(3)	1.1(1)	0
61	213	1.3(1)	1.2(1)	0.62
61	36	1.3(1)	1.2(1)	0.5
62	136	1.6(1)	1.5(1)	0.2
67	98	1.0(1)	1.1(1)	0.15
69	28	1.5(1)	1.4(1)	0.39
82*	36	1.2(2)	1.2(1)	0
89	72	1.4(1)	1.3(1)	0.15
89	48	1.5(1)	1.3(1)	0.2
89	28	1.2(1)	1.3(1)	0.16
91	15	1.4(1)	1.4(1)	0.65
92*	36	1.8(2)	1.3(1)	0
92	28	1.3(1)	1.3(1)	0.42
94*	48	1.6(1)	1.3(1)	0
94*	98	1.5(2)	1.0(1)	0
94	15	1.5(1)	1.5(1)	0.15
105	28	1.5(1)	1.5(1)	0.45
110	28	1.2(1)	1.4(1)	0.18
116	15	1.2(1)	1.3(1)	0.04
122	15	1.5(1)	1.4(1)	0.78
125	28	1.4(1)	1.4(1)	0.88
133	98	1.7(1)	1.2(1)	0.02
162	15	1.2(1)	1.3(1)	0.48
181	15	1.2(2)	1.1(1)	0.1
197	15	1.2(2)	1.2(1)	0.58
201*	15	1.3(2)	1.1(1)	0
262	150	1.3(8)	1.8(1)	0.04
264	1428	1.5(2)	1.7(1)	0.12
269	122	1.6(2)	1.7(1)	0.02
279	550	1.5(2)	1.5(1)	0.22
293*	3503	1.5(1)	1.5(1)	0
300	550	1.5(1)	1.6(1)	0.41
300	150	1.7(1)	1.7(1)	0.17
306*	150	1.5(1)	1.4(1)	0
317	150	1.8(2)	1.6(1)	0.22
318	150	1.5(2)	1.4(1)	0.04
327	1503	1.3(1)	1.4(1)	0.19
327	150	1.6(1)	1.6(1)	0.25
331	150	1.6(2)	1.6(1)	0.29
332	1574	1.6(2)	1.9(1)	0.15

Table S3: BM data set. Each row corresponds to one of the 52 agents who have bid at least 100 times in the same auction. We report the id of the auction a, the id of the agent u, the exponent α calculated with the least square method, the exponent α' calculated with the maximum likelihood method and the p-value. Entries with low p-values are marked with *. In the 79% of the cases we find a p-value larger than 0, which indicates that our model well describe the time series.

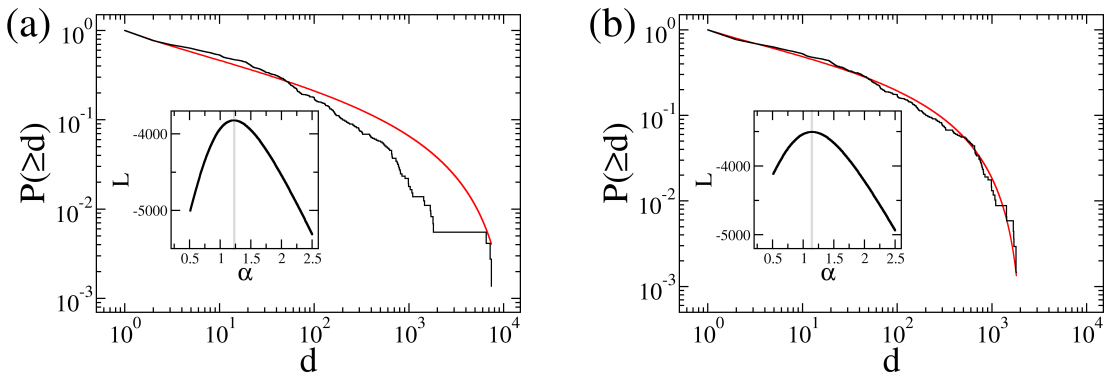

Figure S18: Example of the maximum likelihood method for the determination of the exponent α' of the Lévy flight. We consider the time series of agent 1632 in auction 19 of the UBH data set (the same appearing in Figure S2). In panel a, we set $M = 13\,000$ which is the value of the maximum bid amount that was allowed in the auction. The best exponent $\alpha' = 1.2(1)$ is obtained by looking at the maximum of the log-likelihood as it is shown in the inset. The comparison between the cumulative distribution of the jump lengths expected from the model (red line) and the one calculated over the time series (black) do not well agree. It seems that the "effective" bound is smaller than the real one. In panel b, we set $M = 2\,200$ and consider only bid values smaller than this bound. On the new time series, we perform a maximum likelihood fit finding $\alpha' = 1.1(1)$. The theoretical expectation (red line) and the one obtained from the time series (black line) are now very similar yielding a p-value equal to 0.1.

2. Another maximum likelihood fit

Since the upper-bound M is agent dependent, we perform an additional analysis where the upper bound M is not directly taken from the data, but used as a parameter for the fit. For each agent, we let the parameter M vary only in the range for which at least the 90% of the bids values are below M. Indicate with $\tilde{T}$ the number of bids below the threshold M. We then find α' identifying the maximum of the likelihood function and calculate the p-value as described so far. We consider the best value of M as the one which maximizes the product $\tilde{T} \times p$. Figures S19, S20 and S21 report the best fit for the same agents analyzed in Figures S5, S6 and S7 for UBH data set, while Figures S22, S23 and S24 are the analogous of Figures S8, S9 and S10 for BM data set. For completeness, we report in Tables S4 and S5 the results obtained with the maximum likelihood fit where M is used as parameter of the fit. The best exponents α' are still consistent with those reported in Tables S2 and S3, but the p-values result much increased.

a	u	α	α'	M	p
1^*	23	1.6(1)	1.4(1)	490	0.00
1	81	1.2(1)	1.2(1)	2220	0.26
100	1715	1.6(2)	1.0(1)	150	0.15
100	81	1.5(2)	1.3(1)	480	0.01
104	3093	1.7(3)	1.0(1)	70	0.51
108	134	1.7(1)	1.3(1)	70	0.09
14	134	1.2(1)	1.1(1)	530	0.40
14	81	1.9(2)	1.3(1)	870	0.01
15	423	1.6(4)	1.2(1)	120	0.53
179	3663	1.8(1)	1.3(2)	70	0.35
19	1	1.3(1)	1.3(1)	3050	0.29
19	1313	1.2(1)	1.1(1)	1650	0.50
19	134	1.2(1)	1.0(1)	2320	0.19
19	1433	1.1(1)	0.9(1)	1840	0.99
19	1448	1.4(1)	1.1(1)	2480	0.08
19	1558	1.1(1)	1.2(1)	2290	0.93
19	1576	1.0(1)	0.9(1)	9580	0.34
19	1601	1.4(1)	1.2(1)	480	0.09
19	1632	1.4(1)	1.1(1)	2210	0.13
19^*	1640	1.3(1)	1.2(1)	3080	0.00
19	1642	1.3(1)	1.2(1)	3200	0.45
19^*	1644	1.4(1)	1.2(1)	3010	0.00
19	1645	1.4(1)	1.1(1)	1750	0.03
19	3	1.2(1)	1.3(1)	3310	0.91
19	363	1.2(1)	0.9(1)	890	0.20
19	434	1.1(1)	1.1(1)	1750	0.77
19	438	1.5(1)	0.9(1)	2120	0.43
20	617	1.6(2)	1.3(1)	200	0.09
22	134	1.2(1)	1.3(1)	1000	0.96
44	433	1.1(1)	1.6(1)	3340	0.08
46	2003	1.3(3)	1.4(1)	110	0.03
5	128	1.6(1)	1.4(1)	1830	0.01
62	2392	1.3(3)	1.3(1)	130	0.52
71^*	324	1.6(2)	1.4(1)	860	0.00
73	1640	1.5(2)	1.4(1)	1920	0.27
73	1715	1.5(1)	1.2(1)	140	0.68
79	134	1.6(2)	1.3(1)	120	0.21
91	1715	1.5(2)	1.3(1)	70	0.67
97	1715	1.6(2)	1.2(1)	80	0.19

Table S4: UBH data set. Each row corresponds to one of the 39 agents who have bid at least 50 times in the same auction. We report the id of the auction a, the id of the agent u, the exponent α calculated with the least square method, the exponent α' calculated with the maximum likelihood method, the best value of the upper bound M and the p-value. Entries with low p-values are marked with *. In the 90% of the cases we find a p-value larger than 0, which indicates that our model well describe the time series.

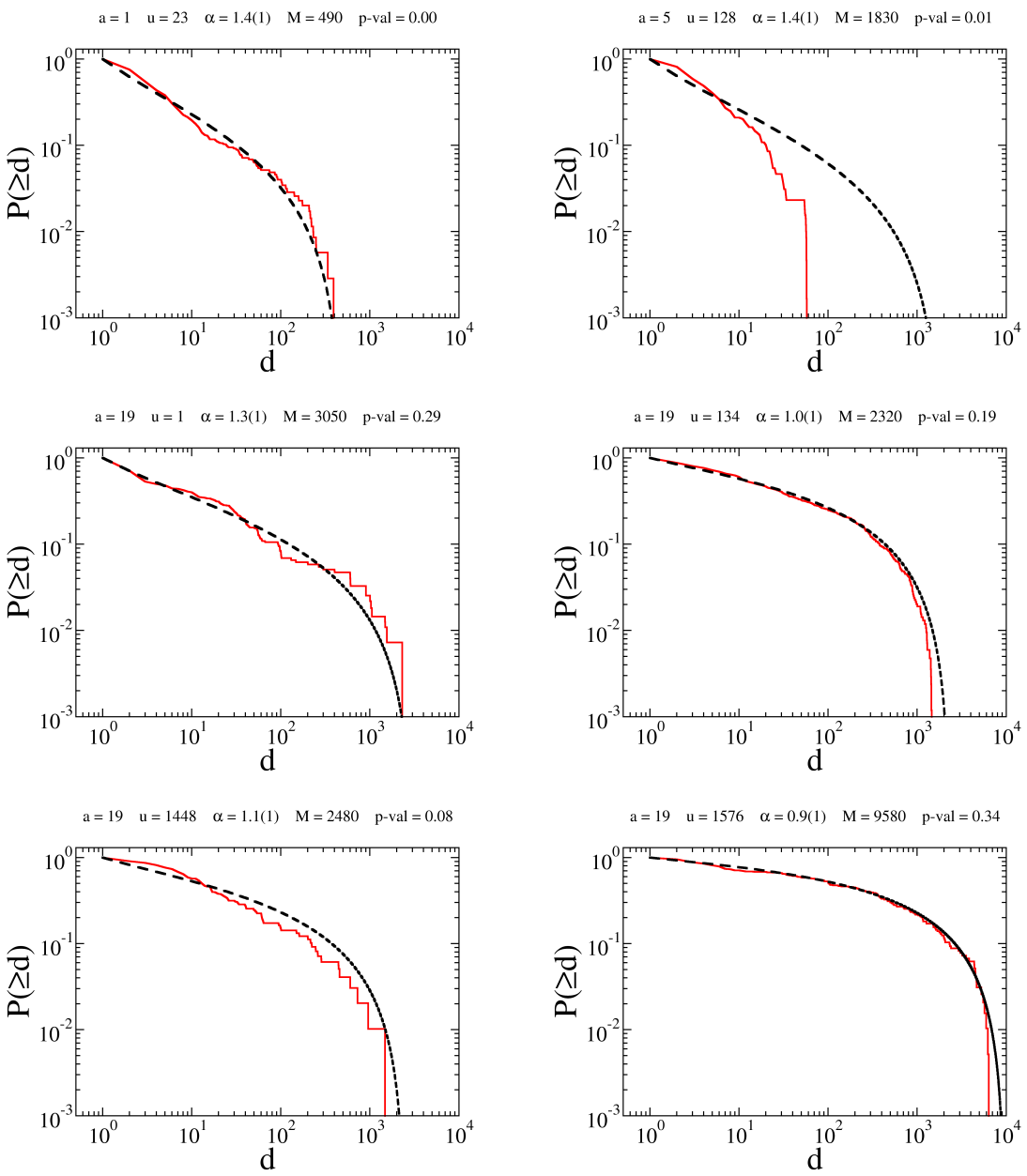

Figure S19: UBH data set. Cumulative distribution function $P(\geq d)$ measured for agent u in auction a (red full line) compared with the theoretical distribution (black dashed line). We show several $P(\geq d)$s for different pairs u and a. We report also the best value of the upper bound M and the p-value associated with our fit.

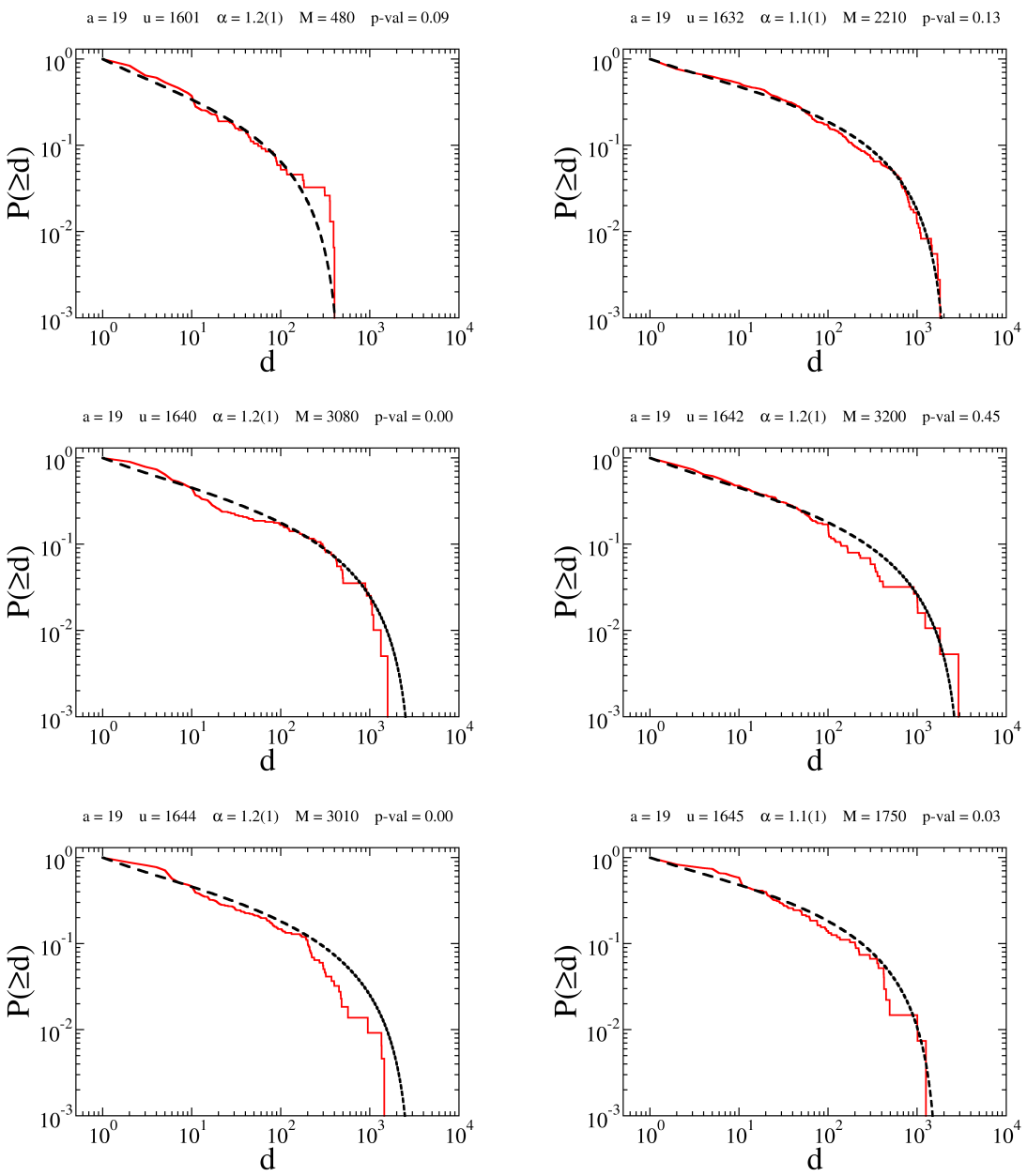

Figure S20: UBH data set. Same as Figure S19.

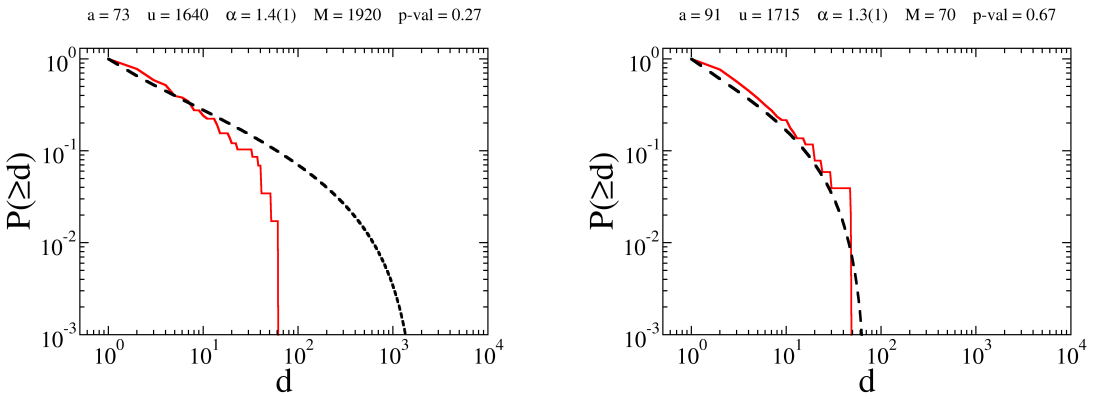

Figure S21: UBH data set. Same as Figure S19 and S20.

a	u	α	α'	M	p
11	28	1.1(2)	1.4(1)	1290	0.23
13*	48	1.5(1)	1.2(1)	570	0.00
13	28	1.3(1)	1.3(1)	310	0.15
15	11	1.8(3)	1.3(1)	180	0.23
15	36	2.0(1)	1.5(1)	200	0.19
28	28	1.4(1)	1.4(1)	530	0.53
32*	150	1.2(6)	1.0(1)	160	0.00
39	48	1.3(1)	1.3(1)	170	0.02
47	28	1.1(1)	1.2(1)	320	0.59
50	48	1.5(1)	1.3(1)	600	0.38
52	28	1.2(2)	1.4(1)	2790	0.11
55	15	1.3(1)	1.3(1)	250	0.68
55*	150	1.2(3)	1.1(1)	220	0.00
61	213	1.3(1)	1.3(1)	220	0.74
61	36	1.3(1)	1.2(1)	140	0.91
62	136	1.6(1)	1.5(1)	180	0.45
67	98	1.0(1)	1.0(1)	210	0.83
69	28	1.5(1)	1.4(1)	1840	0.37
82	36	1.2(2)	1.2(1)	360	0.01
89	72	1.4(1)	1.3(1)	330	0.30
89	48	1.5(1)	1.3(1)	230	0.42
89	28	1.2(1)	1.3(1)	1580	0.17
91	15	1.4(1)	1.4(1)	180	0.87
92	36	1.8(2)	1.3(1)	130	0.04
92	28	1.3(1)	1.4(1)	910	0.46
94	48	1.6(1)	1.2(1)	310	0.18

a	u	α	α'	M	p
94	98	1.5(2)	0.9(1)	280	0.03
94	15	1.5(1)	1.4(1)	290	0.28
105	28	1.5(1)	1.5(1)	1310	0.59
110	28	1.2(1)	1.4(1)	2870	0.36
116	15	1.2(1)	1.3(1)	3050	0.13
122	15	1.5(1)	1.4(1)	470	0.95
125	28	1.4(1)	1.4(1)	790	0.89
133	98	1.7(1)	1.2(1)	140	0.15
162	15	1.2(1)	1.4(1)	3270	0.54
181	15	1.2(2)	1.0(1)	250	0.34
197	15	1.2(2)	1.2(1)	180	0.79
201	15	1.3(2)	1.1(1)	110	0.43
262	150	1.3(8)	1.8(1)	1200	0.08
264	1428	1.5(2)	1.7(1)	1610	0.16
269	122	1.6(2)	1.7(1)	970	0.02
279	550	1.5(2)	1.6(1)	2600	0.32
293	3503	1.5(1)	1.5(1)	2030	0.01
300	550	1.5(1)	1.5(1)	290	0.68
300	150	1.7(1)	1.7(1)	1900	0.26
306*	150	1.5(1)	1.4(1)	740	0.00
317	150	1.8(2)	1.6(1)	260	0.38
318	150	1.5(2)	1.4(1)	610	0.05
327	1503	1.3(1)	1.4(1)	230	0.54
327	150	1.6(1)	1.5(1)	290	0.46
331	150	1.6(2)	1.6(1)	1500	0.42
332	1574	1.6(2)	1.9(1)	1140	0.15

Table S5: BM data set. Each row corresponds to one of the 52 agents who have bid at least 100 times in the same auction. We report the id of the auction a, the id of the agent u, the exponent α calculated with the least square method, the exponent α' calculated with the maximum likelihood method, the best value of the upper bound M and the p-value. Entries with low p-values are marked with *. In the 92% of the cases we find a p-value larger than 0, which indicates that our model well describe the time series.

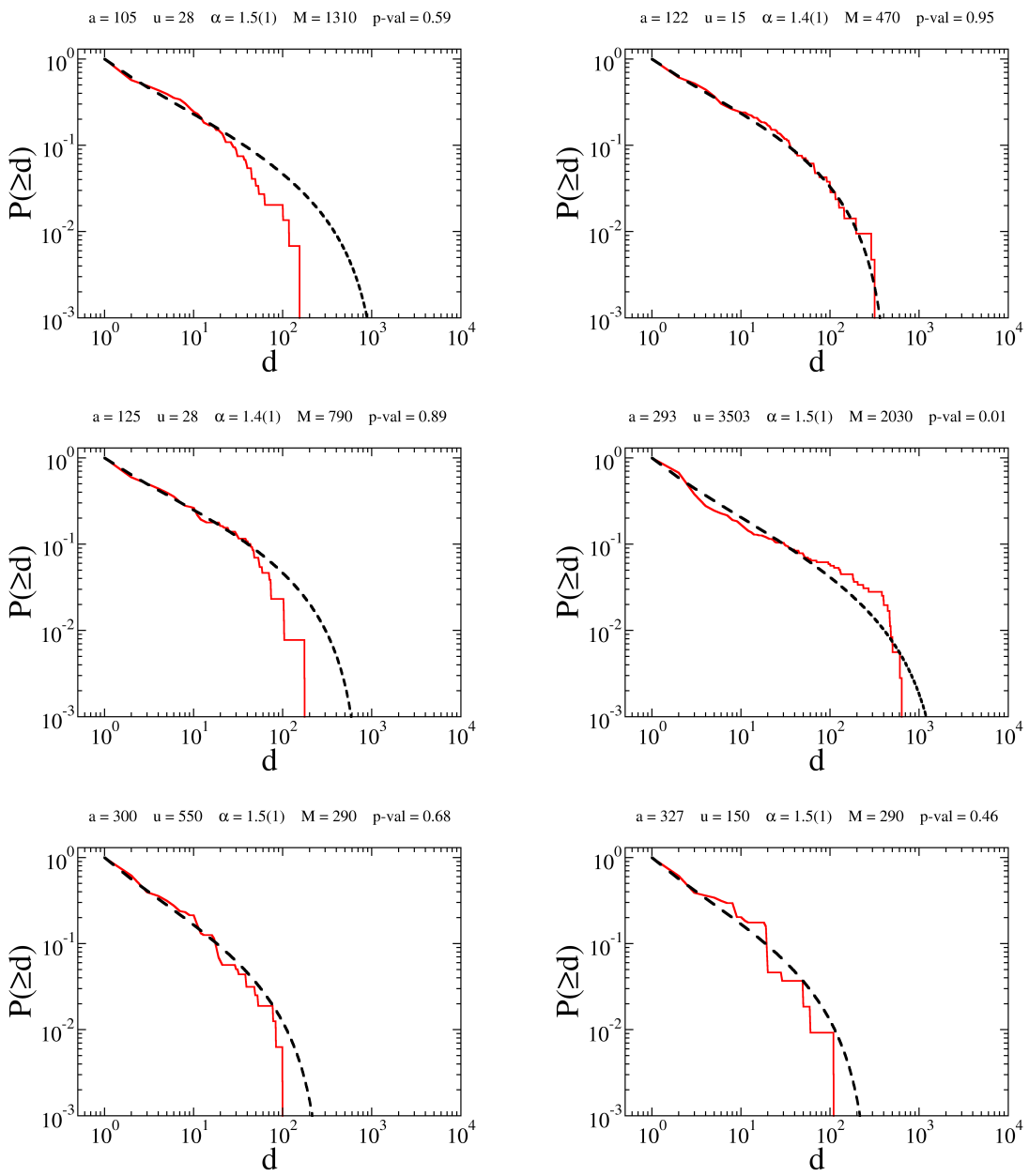

Figure S22: BM data set. Cumulative distribution function $P(\geq d)$ measured for agent u in auction a (red full line) compared with the theoretical distribution (black dashed line). We show several $P(\geq d)$s for different pairs u and a. We report also the best value of the upper bound M and the p-value associated with our fit.

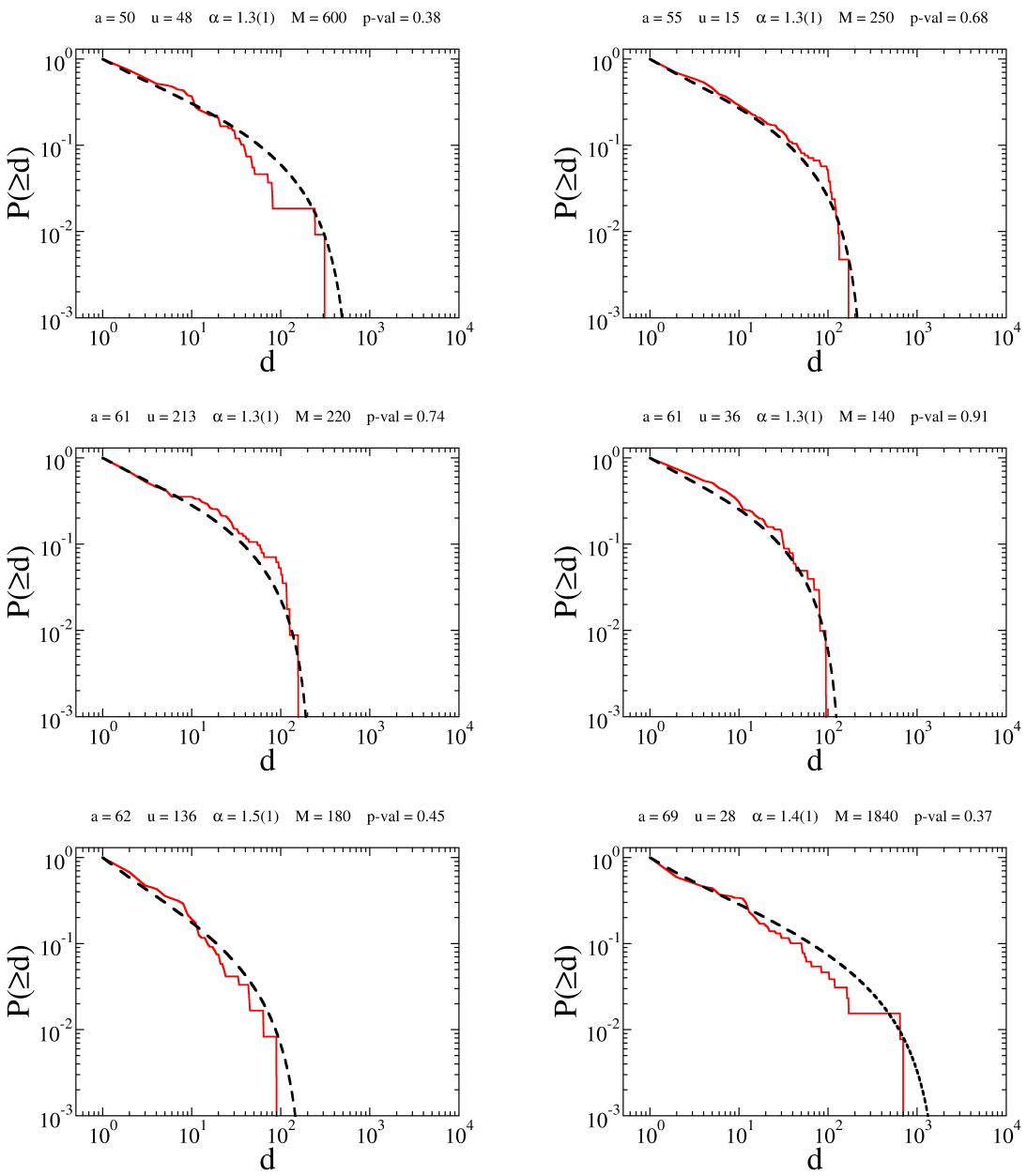

Figure S23: BM data set. Same as Figure S22.

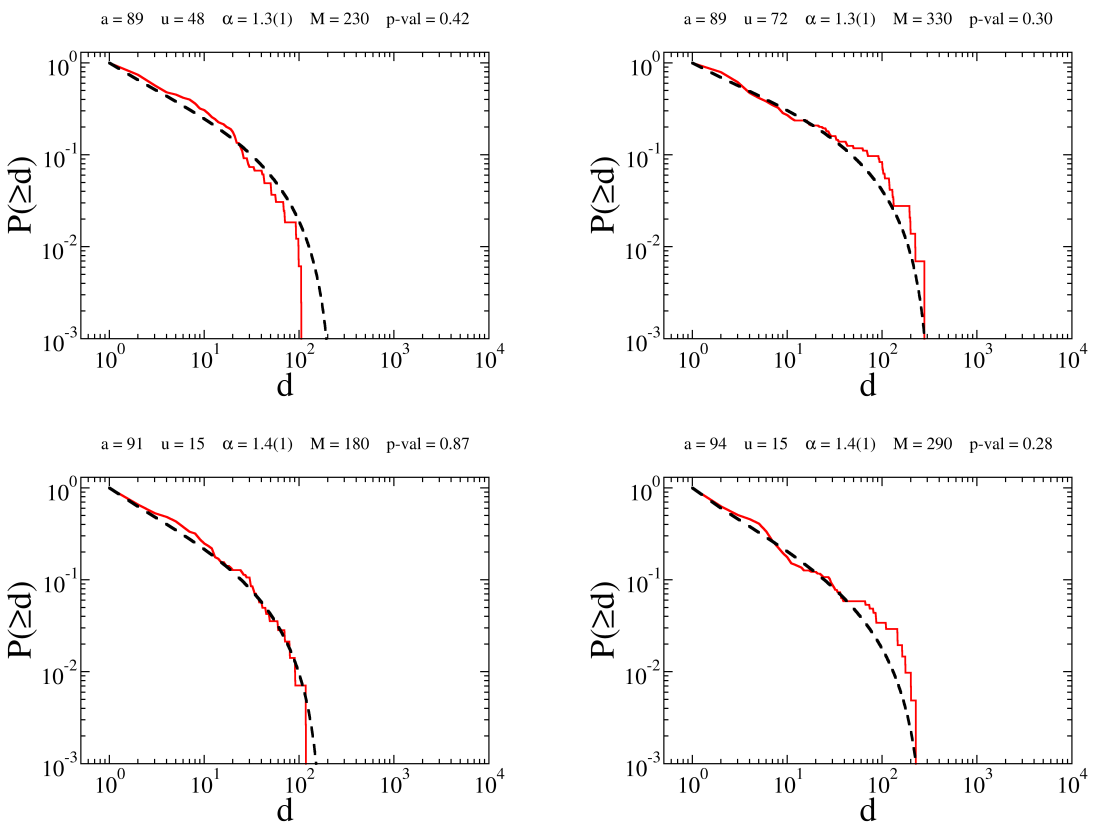

Figure S24: BM data set. Same as Figure S22 and S23.

3. *Probability distribution of the Lévy flight exponents*

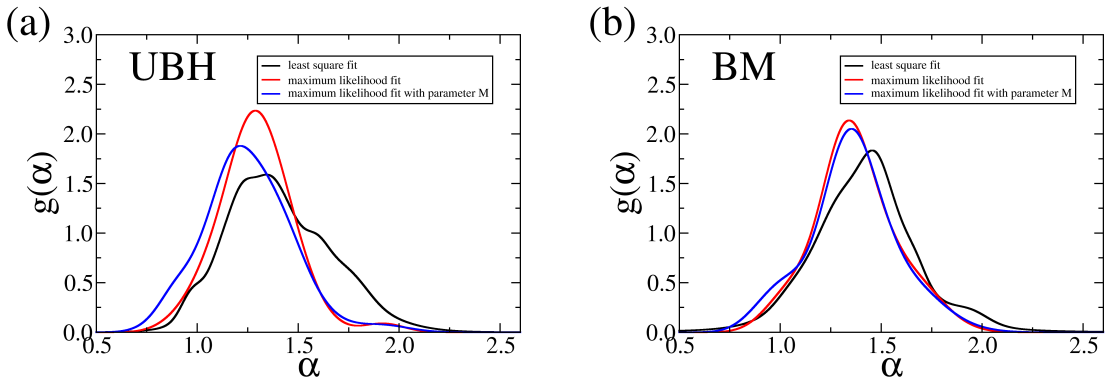

Figure S25: The pdf $g(\alpha)$ of the exponents calculated with the three fitting methods. The pdfs corresponding to the maximum likelihood fit, where M is a parameter of the fit, are the same as those appearing in Figs. 2D and 2E of the main text. The distributions are characterized by the following values of the mode α_b, average $\langle\alpha\rangle$ and variance σ. UBH data set: for least square fit we have $\alpha_b = 1.34$, $\langle\alpha\rangle = 1.40$, $\sigma = 0.26$; for maximum likelihood fit we have $\alpha_b = 1.28$, $\langle\alpha\rangle = 1.29$, $\sigma = 0.20$; for maximum likelihood fit with additional fitting parameter M we have $\alpha_b = 1.21$, $\langle\alpha\rangle = 1.26$, $\sigma = 0.23$. BM data set: for least square fit we have $\alpha_b = 1.46$, $\langle\alpha\rangle = 1.42$, $\sigma = 0.27$; for maximum likelihood fit we have $\alpha_b = 1.34$, $\langle\alpha\rangle = 1.37$, $\sigma = 0.21$; for maximum likelihood fit with additional fitting parameter M we have $\alpha_b = 1.35$, $\langle\alpha\rangle = 1.36$, $\sigma = 0.23$.

As a final result, we compute the distribution $g(\alpha)$ of the exponents measured for single agents in single auctions. We still consider only agents who have performed at least $T = 50$ bids in a single auction in UBH data set and those with at least $T = 100$ in the BM data set. Assuming that the best estimation of the exponent of agent u is α_u and the associated error of the measurement is $\Delta\alpha_u$, the empirical distribution of the exponents is calculated as

$$g(\alpha) = C^{-1} \sum_u \frac{1}{\Delta\alpha_u} e^{-(\alpha_u-\alpha)^2 / \left[2(\Delta\alpha_u)^2\right]} \ , \tag{S4}$$

where $C = \int d\alpha \ \sum_u \frac{1}{\Delta\alpha_u} \ e^{-(\alpha_u-\alpha)^2 / \left[2(\Delta\alpha_u)^2\right]}$ is the proper normalization constant. The resulting pdfs are reported in Fig. S25.